



Progress on the synthesis of superheavy nuclei

Ming-Hao Zhang^{1,2} · Zhi-Yuan Zhang³ · Zai-Guo Gan³ · Shan-Gui Zhou^{4,5} · Feng-Shou Zhang^{1,2,5}

Received: 18 September 2024 / Revised: 24 December 2024 / Accepted: 25 December 2024 / Published online: 14 August 2025

© The Author(s), under exclusive licence to China Science Publishing & Media Ltd. (Science Press), Shanghai Institute of Applied Physics, the Chinese Academy of Sciences, Chinese Nuclear Society 2025

Abstract

The synthesis of superheavy nuclei remains a critical area of research in nuclear physics, with the aim of extending the periodic table and deepening our understanding of the properties of nuclei. This review provides a comprehensive overview of the latest advancements in superheavy nuclei synthesis, focusing on both the experimental and theoretical developments. We discuss the primary synthesis methods, including early fusion reactions with light nuclei, cold fusion reactions using lead and bismuth targets, and hot fusion reactions involving ⁴⁸Ca projectiles and actinide targets. In addition, we introduce the major experimental facilities and theoretical models currently employed worldwide. This review also summarizes the experimental plans and theoretical predictions for the synthesis of new superheavy elements. Furthermore, we discuss future directions, including the potential of employing heavier projectiles, radioactive beam-induced reactions, and multi-nucleon transfer reactions, which may offer new pathways for discovering unknown superheavy nuclei.

Keywords Heavy ion physics · Superheavy nuclei · Reaction mechanism · Fusion reactions · Multi-nucleon transfer reaction

1 Introduction

There are 288 naturally existing nuclei on earth, with ²³⁸U being the heaviest among them. Transuranium nuclei, with atomic numbers greater than 92, can only be produced through nuclear reactions [1–3]. The first transuranium

This work was supported by the National Key R&D Program of China (No. 2023YFA1606401), and the National Natural Science Foundation of China (Nos. 12135004, 11635003, 11961141004, 12375118, and 12435008), the National Key R&D Program of China (Nos. 2023YFA1606500, 2023YFA1606501, 2023YFA1606504), the Strategic Priority Research Program of Chinese Academy of Sciences (No. XDB34010000), the Major State Basic Research Development Program of China (2023YFA1606503), and the CAS Strategic Priority Research Program (XDB34010000).

✉ Feng-Shou Zhang
fszhang@bnu.edu.cn

¹ The Key Laboratory of Beam Technology of Ministry of Education, School of Physics and Astronomy, Beijing Normal University, Beijing 100875, China

² Institute of Radiation Technology, Beijing Academy of Science and Technology, Beijing 100875, China

³ Institute of Modern Physics, Chinese Academy of Sciences, Lanzhou 730000, China

nucleus, ²³⁹Np, was discovered in 1940 among the fission products resulting from bombardment of ²³⁸U with thermal neutrons [4]. Since then, nuclear physicists have successfully synthesized 26 transuranium elements artificially by utilizing several types of nuclear reactions. Among these artificial nuclei, transactinide nuclei with $Z \geq 104$ are known as superheavy nuclei (SHNs) [5–7]. These nuclei are located in the upper-right corner of the nuclear chart and exhibit extreme instability and short half-lives. Nevertheless, the synthesis and study of SHNs are crucial for advancing our understanding of the fundamental properties of nuclear forces, validating nuclear structural models, and extending the periodic table of elements.

⁴ CAS Key Laboratory of Theoretical Physics, Institute of Theoretical Physics, Chinese Academy of Sciences, Beijing 100190, China

⁵ Center of Theoretical Nuclear Physics, National Laboratory of Heavy Ion Accelerator of Lanzhou, Lanzhou 730000, China

Although the SHN region lies at the limits of Coulomb stability, the shell structure effects can influence the fission barrier, thereby contributing to the existence of SHNs. Following the approach proposed by Strutinsky, which involves introducing shell corrections to the liquid-drop model, an “island of stability” at $Z = 114$ and $N = 184$ was predicted separately by Sobiczewski et al. and Meldner [8–12]. Further predictions from various microscopic approaches, such as the Skyrme–Hartree–Fock and relativistic mean-field methods, suggest that this “island of stability” could be located at $Z = 114, 120, 124$ or 126 and $N = 172$ or 184 [13–15, 15–20]. These theoretical predictions are supported by the observed increase in α -decay half-lives of isotopes with increasing neutron number [8, 21].

The primary mechanism for synthesizing SHNs involves fusion reactions using stable beams and long-lived targets. Early fusion reactions utilizing lighter projectiles and actinide targets were selected to produce superheavy elements (SHEs) with $Z = 93 – 106$ at LBNL and JINR [22–26]. Subsequent advancements in cold fusion reactions employing ^{208}Pb or ^{209}Bi targets facilitated the synthesis of SHEs with $Z = 107–113$ at GSI and RIKEN [27, 28]. In contrast, hot fusion reactions using ^{48}Ca beams and actinide targets conducted in JINR at Dubna led to the successful synthesis of SHEs with $Z = 114–118$ [29–33]. Currently, the synthesis of new SHEs with $Z = 119–122$ represents a highly competitive frontier in nuclear research.

This review provides a comprehensive overview of the current state of research on the synthesis of SHNs, focusing on both experimental accomplishments and theoretical advancements. We discuss the latest achievements and breakthroughs in the synthesis of SHN, experimental facilities, and theoretical methods employed. Furthermore, this review discusses the challenges encountered in synthesizing new SHN and explores the potential directions for future research.

This article is organized as follows: In Sect. 2, we introduce the discovered SHN and the methods used for their synthesis. Section 3 covers the current experimental facilities, including both existing and underconstruction accelerators and separators. In Sect. 4, we discuss the widely applied microscopic and phenomenological models used in theoretical predictions. Section 5 reviews the latest experimental and theoretical advancements in the synthesis of new SHEs. Section 6 addresses the current experimental challenges in synthesizing new SHN and explores potential future developments. Finally, Sect. 7 provides a summary of this study.

2 The discovery of superheavy nuclei

2.1 Early fusion reactions with C, N, O, Ne, Mg and Ar beams

There are 3386 discovered nuclei of 118 known elements, including 119 artificial SHNs [34]. The discovery of superheavy isotopes began in 1969 at Berkeley, where the fusion reactions $^{12,13}\text{C} + ^{249}\text{Cf}$ led to the identification of $^{257–259}\text{Rf}$ [22]. By changing the projectile into ^{15}N and ^{18}O , the elements with $Z = 105$ and 106 were also synthesized [23, 24]. JINR also independently produced the 104th and 105th elements via reactions $^{22}\text{Ne} + ^{242}\text{Pu}$, ^{243}Am [25, 26]. Additionally, based on the actinide targets ^{248}Cm and ^{249}Bk , researchers have successfully synthesized new superheavy nuclei $^{260–262}\text{Rf}$ and ^{262}Db [35, 36].

In 2000, the reaction $^{22}\text{Ne} + ^{241}\text{Am}$ was investigated at the Institute of Modern Physics (IMP) in China, leading to the discovery of ^{259}Db [37]. In 2006, using the reaction $^{26}\text{Mg} + ^{248}\text{Cm}$, $^{270,271}\text{Hs}$ were produced at GSI, with $^{266,267}\text{Sg}$ identified in the α -decay descendants [38, 39]. Most recently, in 2024, JINR researchers employed the reaction $^{40}\text{Ar} + ^{238}\text{U}$, resulting in the synthesis of ^{273}Ds [40]. Experimental results suggest that more asymmetric reaction systems can enhance both the fusion probability and evaporation residue (ER) cross sections when forming the same compound nucleus. For instance, in the 5n-emission channel leading to the formation of ^{273}Ds , the ER cross section for the reaction $^{34}\text{S} + ^{244}\text{Pu}$ is 0.4 pb [41], while for the reaction $^{40}\text{Ar} + ^{238}\text{U}$, it is 0.18 pb [40]. Similarly, the fusion cross sections for producing ^{232}Cm and ^{274}Hs via reactions $^{35}\text{Cl} + ^{197}\text{Au}$ and $^{26}\text{Mg} + ^{248}\text{Cm}$ are higher than those produced through reactions $^{40}\text{Ca} + ^{192}\text{Os}$ and $^{36}\text{S} + ^{238}\text{U}$ [42–46].

In the early stages of fusion reactions involving extremely asymmetric reaction partners, the formed compound nuclei possess high excitation energies, requiring the evaporation of three to five neutrons to reach the ground state. However, strong competition from fission during the de-excitation process significantly suppressed the yield of the desired nuclei. The limited atomic number of the light projectiles also constrains the atomic number of the SHE that can be synthesized experimentally. Therefore, there is a need to explore new reaction mechanisms to improve the synthesis efficiency of new elements.

2.2 Superheavy nuclei produced by cold fusion reactions

In 1974, researchers at JINR explored an alternative reaction mechanism to synthesize new SHNs [47]. By

employing $^{206-208}\text{Pb}$ targets and ^{50}Ti and ^{54}Cr projectiles, they discovered new isotopes of $^{255,256}\text{Rf}$ and ^{260}Sg [48, 49]. Because of the reduced mass asymmetry of these reaction systems and the high binding energies of the reaction partners, the excitation energies of the formed compound nuclei were suppressed. This resulted in a de-excitation process requiring the emission of only one or two neutrons, thereby reducing competition from fission. Compared to reactions involving actinide targets and light projectiles, this new reaction mechanism exhibited enhanced ER cross sections. This approach, characterized by low excitation energy and fewer neutron emission, is referred to as “cold fusion reaction”.

Another advantage of cold fusion reactions is that the commonly used ^{208}Pb and ^{209}Bi targets are more readily available in large quantities than actinide targets. In addition, the experimental conditions can be simplified as they are stable target nuclei. Therefore, GSI in Germany had selected this reaction mechanism to investigate the synthesis of new SHEs. In 1981, researchers at GSI managed to synthesize element with $Z = 107$ via the reaction $^{54}\text{Cr} + ^{209}\text{Bi} \rightarrow ^{262}\text{Bh} + \text{n}$ [50]. Following this, through the reactions $^{58}\text{Fe} + ^{208}\text{Pb} \rightarrow ^{265}\text{Hs} + \text{n}$, $^{58}\text{Fe} + ^{209}\text{Bi} \rightarrow ^{266}\text{Mt} + \text{n}$, $^{62,64}\text{Ni} + ^{208}\text{Pb} \rightarrow ^{269,271}\text{Ds} + \text{n}$, $^{70}\text{Zn} + ^{208}\text{Pb} \rightarrow ^{277}\text{Cn} + \text{n}$, the SHEs with $Z = 108-112$ were successfully synthesized [51–55].

Based on the cold fusion reaction, dozens of superheavy nuclei with $Z = 104-110$ were also synthesized in the GSI [54, 56–61]. In addition, Berkely synthesized ^{267}Ds in the 1n-emission channel of the reaction $^{59}\text{Co} + ^{209}\text{Bi} \rightarrow ^{267}\text{Ds} + \text{n}$ [62]. The synthesis of ^{271}Ds via the reaction $^{64}\text{Ni} + ^{208}\text{Pb}$ was also studied by researchers at IMP [63].

In 2004, RIKEN employed the reaction $^{70}\text{Zn} + ^{209}\text{Bi}$ and successfully synthesized the element with $Z = 113$ in the 1n-evaporation channel [27]. However, the ER cross section was only 0.03pb , which is 10^7 times smaller than the ER cross section for synthesizing Bohrium. As shown in Fig. 1, there is an exponentially decreasing trend in the ER cross sections as the proton number of the formed compound nucleus increases [64]. This decrease is primarily due to the strong hindrance to the fusion of colliding nuclei caused by increasing Coulomb repulsion [65], as well as the deviation of the deformed subshell with $Z = 108$ and $Z = 112$ [66, 67]. The synthesis of SHN with $Z \geq 113$ encounters significant challenges owing to the extremely small ER cross sections, which have reached the limitation of experimental detection. In addition, the limited number of neutrons in heavy projectiles results in the formation of compound nuclei closer to the proton drip line, which decreases their stability and makes detection even more challenging.

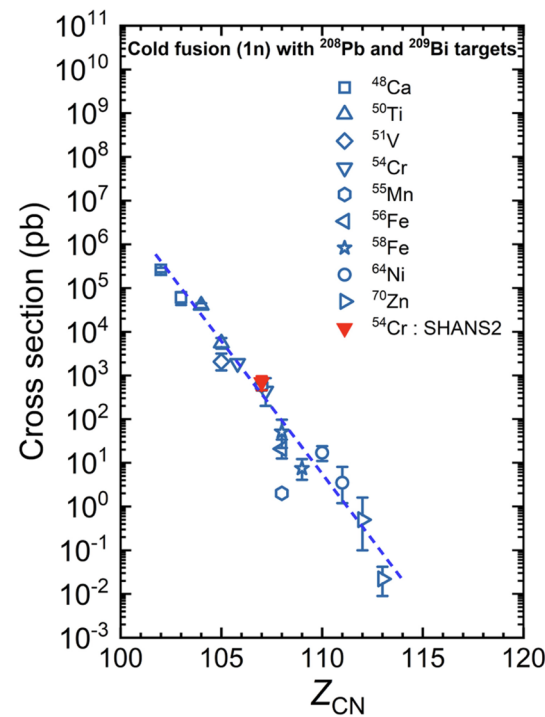


Fig. 1 (Color online) The measured ER cross sections for producing SHN via cold fusion reactions. Open symbols mark the data of the 1n-emission channel in cold fusion reactions based on different projectiles and ^{208}Pb , ^{209}Bi targets. The solid symbol represent data provided by SHANS2 experiments. Dashed line is drawn to guide the eye. Reproduced from Ref. [64]

2.3 Superheavy nuclei produced by ^{48}Ca -induced hot fusion reactions

To reduce the hindrance caused by Coulomb repulsion, researchers at JINR explored combinations of ^{48}Ca projectile and actinide targets. The selection of ^{48}Ca as a projectile is due to its doubly magic nature with a high binding energy, which enhances fusion probabilities and lowers the excitation energy of the formed compound nuclei. Moreover, the high neutron excess of ^{48}Ca contributes to the formation of neutron-rich compound nuclei. These neutron-rich nuclei tend to exhibit greater stability due to the reduced Coulomb repulsion among protons, a factor that is particularly crucial for superheavy elements, which possess large atomic numbers and therefore significant Coulomb forces acting against their stability.

In Table 1, the characteristics of the three types of fusion reaction are presented. Although the excitation energies in hot fusion reactions are higher than those in cold fusion reactions, leading to a lower survival probability of compound nuclei, the fusion probability in hot fusion reactions is enhanced by the high mass asymmetry of the reaction systems. Additionally, the neutron-rich

Table 1 Comparative summary of early fusion, cold fusion, and hot fusion reactions

Aspect	Early fusion reactions	Cold fusion reactions	Hot fusion reactions
Projectile	Light nuclei with $Z = 6\text{--}18$	Heavy nuclei with $Z = 22\text{--}30$	Double magic nucleus ^{48}Ca
Target	Actinide targets	Pb or Bi targets	Actinide targets
Excitation energy	Higher, leading to 3–5 neutron emission	Lower, leading to 1–2 neutron emission	Higher, leading to 3–5 neutron emission
ER cross section range	From microbarn range to picobarn range	From microbarn range to femtobarn range	Picobarn range
Character of products	Neutron-deficient, $Z = 104\text{--}110$, less stable	Neutron-deficient, $Z = 104\text{--}113$, less stable	Neutron-rich, $Z = 104\text{--}118$, potentially more stable
Successful synthesis	Elements 104 to 106	Elements 107 to 113	Elements 114 to 118

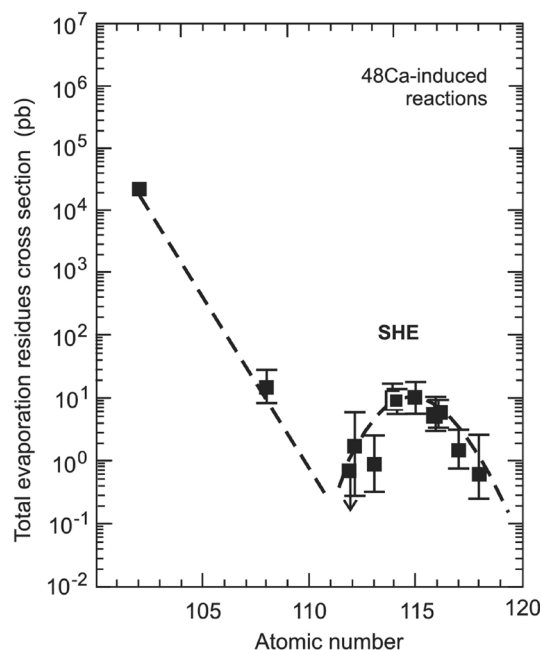


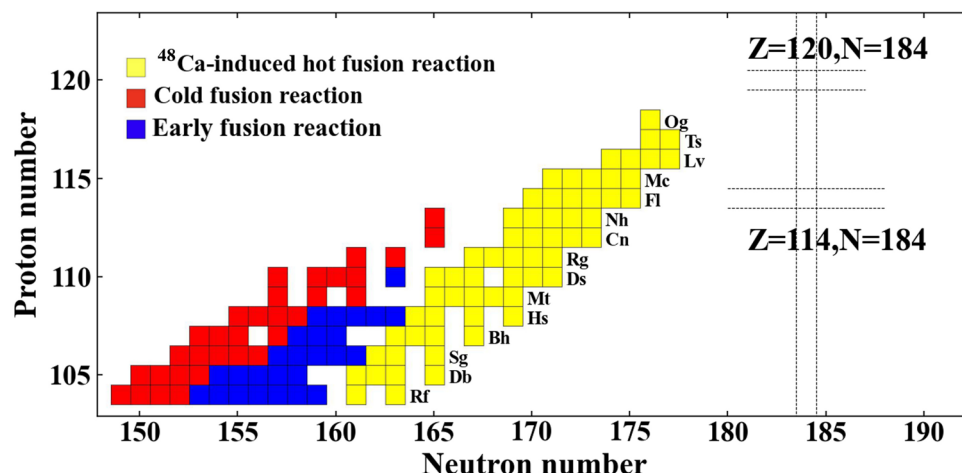
Fig. 2 (Color online) The measured ER cross sections for producing SHN via reactions induced by the ^{48}Ca beam. The measured data are shown by solid squares. Dashed line is drawn to guide the eye. Reproduced from Ref. [65]

Fig. 3 (Color online) The superheavy nuclei chart. The yellow, red and blue squares denote SHN synthesized via ^{48}Ca -induced hot fusion reaction, cold fusion reaction and early fusion reaction, respectively. The predicted centers of the “island of stability” are indicated by the black dashed lines

projectile ^{48}Ca results in the formation of compound nuclei with a greater neutron excess. The increased neutron-to-proton ratio in these compound nuclei enhanced their binding energy and stability.

The first hot fusion reactions began with the ^{244}Pu target, leading to the discovery of three isotopes of Flerovium, $^{287\text{--}289}\text{Fl}$ [68]. Subsequently, elements with $Z = 115\text{--}118$ were synthesized using targets of ^{243}Am , ^{248}Cm , ^{249}Bk , and ^{249}Cf , thereby completing the seventh period of the periodic table [29, 31–33, 69]. The maximal ER cross sections for the hot fusion reactions are shown in Fig. 2. This reveals that the maximal ER cross sections increase as the proton number of the formed compound nucleus approaches the predicted shell closure at $Z = 114$, which is consistent with the increased fission barrier height predicted by macro-microscopic theory [70, 71]. Moreover, a new isotope of element 113 was discovered through the reaction $^{48}\text{Ca} + ^{237}\text{Np}$, with an ER cross section of 0.9 pb, which is an order of magnitude higher than that for synthesizing element 113 via cold fusion reactions [72].

Figure 3 illustrates the SHNs synthesized through three types of fusion reactions, including those identified in the decay products. Compared with the other two types of fusion reactions, hot fusion reactions are particularly effective in synthesizing nuclei with higher proton numbers and greater



neutron excess. Consequently, hot fusion reactions have become increasingly favored for the synthesis of new SHNs in recent years.

In 2021, GSI investigated the reaction $^{48}\text{Ca} + ^{242,244}\text{Pu}$ and discovered a new isotope, ^{280}Ds , from decay descendants [73]. In 2022, researchers at Dubna identified ^{286}Mc in the 5n-emission channel of the reaction $^{48}\text{Ca} + ^{243}\text{Am}$ [74]. In 2023, they explored the reaction $^{48}\text{Ca} + ^{232}\text{Th}$ and discovered a new isotope ^{276}Ds , with ^{272}Hs and ^{268}Sg identified among the decay products [75]. This reaction was reattempted in 2024, leading to the discovery of ^{275}Ds in the 5n-emission channel [40].

3 Experimental facilities

Modern heavy ion research centers such as HIRFL in China, RIKEN in Japan, GSI in Germany, JINR in Russia, GANIL in France, LBNL, and LLNL in the USA have made significant progress in the synthesis of new isotopes with $Z \leq 118$ [27, 63, 67, 74, 76–80]. The largest heavy ion research facility in China is HIRFL at IMP [81, 82]. Its accelerator system consists of two cyclotrons (SFC and SSC), a synchrotron (CSRm), and a storage ring spectrometer (CSRe), as depicted in Fig. 4. Typically, the SFC is used as an injector for the SSC. Ions generated by the ion sources are first accelerated by the SFC and then injected into the SSC for further acceleration. The heavy ions provided by both cyclotrons can be accumulated, cooled, and accelerated in CSRm, then extracted to produce radioactive ion beams (RIB) or highly charged heavy ions. These secondary beams are accepted and stored in CSRe for various internal target experiments. In recent years, researchers at IMP have successfully synthesized 38 new nuclei, including 23 heavy and superheavy nuclei, based on HIRFL and other accelerators [83–95].

The UNILAC installed in 1975 at GSI is capable of accelerating all ion species from protons to uranium with energies

ranging from 1.4 MeV/u to 11.4 MeV/u [96, 97]. Over the past 40 years, experiments using beams from UNILAC have successfully produced elements with $Z = 107$ –112 and more than four hundred new isotopes [5]. Additionally, UNILAC along with the Heavy Ion Synchrotron SIS18, will serve as a high-current heavy ion injector for the new Facility for Antiproton and Ion Research (FAIR) Synchrotron SIS100 [98, 99].

The linear accelerator RILAC, constructed in 1975 at RIKEN, successfully synthesized approximately 200 new isotopes and made significant contributions to the synthesis and discovery of Nihonium [5, 100]. To facilitate the synthesis of new SHEs with $Z = 119$, RILAC was upgraded to a superconducting linear accelerator system (SRILAC) in 2020 [101, 102]. The beam energy was increased from 5.5 MeV/u to 6.5 MeV/u, enabling SRILAC to play a major role in the synthesis of even heavier new elements.

The Flerov Laboratory of Nuclear Reactions (FLNR) in JINR has produced more than 200 new isotopes using two primary cyclotrons, DC-280 and U-400 [69, 103]. The U-400 accelerator, established in 1979 and continuously upgraded, plays a significant role in the synthesis of elements with $Z = 113$ –118. To further explore the SHE region, DC-280 was developed in 2018, offering beam energies ranging from 4 MeV/u to 8 MeV/u and beam intensities up to 10 μA , making it particularly suitable for the synthesis of new SHN [104–106].

The 88-inch Cyclotron Facility at LBNL was first commissioned in 1961 and has been in operation for over six decades. It has played a crucial role in the discovery of more than 600 isotopes [5, 100, 107]. In 2022, the construction of the Facility for Rare Isotope Beams (FRIB) was completed. The superconducting driver linac in the recently developed FRIB at MSU can accelerate the ^{238}U isotope with a beam energy greater than 200 MeV/u, which provides access to the production of thousands of new nuclei [108–111].

Progressive and expansive research in nuclear physics continues to drive the upgradation and modernization of accelerators. The High-Intensity Heavy Ion Accelerator Facility (HIAF) is a next-generation storage ring-based heavy ion facility developed by IMP, with expected completion by 2025 [112, 113]. HIAF integrates a linear accelerator and a synchrotron accelerator to deliver high-energy heavy ion beams ranging from hydrogen to uranium. The principal goal of HIAF is to synthesize new superheavy nuclei and elements [114, 115]. In parallel, other advanced accelerator facilities, such as the FAIR SIS 100 at GSI, NICA-Booster in Dubna, and EURISOL in Europe, are currently under design and construction [116–118]. The comprehensive beam parameters for these facilities are detailed in Ref. [114].

For the synthesis of a new SHN, the expected ER cross sections are on the order of picobarns, with half-lives ranging from microseconds to several days [119]. The

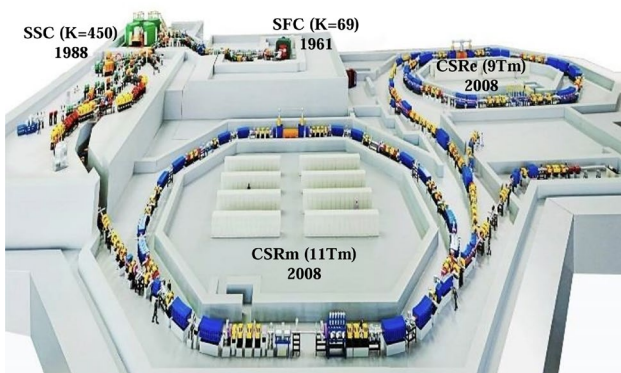


Fig. 4 (Color online) The layout of HIRFL complex. Reproduced from Ref. [82]

predominant decay modes for these unknown nuclei are predicted to be alpha decay and spontaneous fission. Therefore, decay products are typically separated and implanted into radiation-sensitive Si detectors. The detection of rare alpha-decay events from the synthesized SHN is then carried out against a significant background of side reaction products.

Currently, several kinematic separators have been employed in the study of heavy nuclei. Velocity filter SHIP at GSI and SHELS at JINR are notable examples [120, 121]. These facilities specialize in the separation and identification of heavy nuclei fragments using velocity filtering techniques. In addition, gas-filled magnetic separators, such as DGFRS-2 at JINR, TASCA at GSI, BGS at LBNL, GARIS-II at RIKEN, and SHANS at HIRFL, are employed to enhance the separation and detection of SHEs [122–127]. The detailed design of gas-filled recoil separators is described in Ref. [77]. These separators enable effective separation and high-sensitivity detection, which are critical for advancing the SHE research.

In recent years, the next generation of separators has been gradually put into operation. The GARIS-III at RIKEN was completed as part of an upgrade project in 2020. With enhanced resolution and advanced detector arrays, the aim was to investigate reactions with ER cross sections as low as 10 fb [102, 128]. In 2022, the CAFE2 Program at IMP initiated the development of a new gas-filled recoil separator, SHANS2, as illustrated in Fig. 5. Through a series of performance tests involving the reactions $^{40}\text{Ar} + ^{175}\text{Lu}$, $^{40}\text{Ar} + ^{169}\text{Tm}$, $^{40}\text{Ca} + ^{169}\text{Tm}$, and $^{55}\text{Mn} + ^{159}\text{Tb}$, SHANS2 demonstrated its effectiveness and reliability, highlighting SHANS2 as a critical tool for advancing research in the field of SHE synthesis [129, 130].

4 Theoretical models

Currently, experiments aimed at investigating superheavy regions encounter several challenges. The target materials available are rare, expensive, and prone to contamination during experiments. Additionally, the limited beam intensity of accelerators requires long irradiation times, and the expected ER cross sections have already reached the detection limits. As a result, it is necessary to develop theoretical models that can provide precise predictions for optimal projectile-target combinations, incident energies, expected yields, and assess the feasibility of experimental plans.

Based on extensive experimental data, two main types of theoretical approaches have been developed to describe fusion-evaporation reactions. One type is the microscopic models, such as the quantum molecular dynamics (QMD) model [131–133] and time-dependent Hartree-Fock (TDHF) theory [134–138]. The other type is the macroscopic phenomenological models, including the fusion-by-diffusion (FBD) model [134, 139, 140], dynamical cluster-decay model (DCM) [141, 142], two-step model [143–146], statistical model [147], multidimensional Langevin-type dynamical equations [148–151], and dinuclear system (DNS) model [9, 152–161].

4.1 Microscopic models

Microscopic models start with basic nucleon-nucleon interactions, often described by effective potentials such as Skyrme potentials. These models require self-consistent field calculations, in which each nucleon moves within the mean field generated by all other nucleons. Microscopic models offer a deep understanding of nucleon behavior and can explain and predict a wide range of nuclear phenomena. However, they often require significant computational

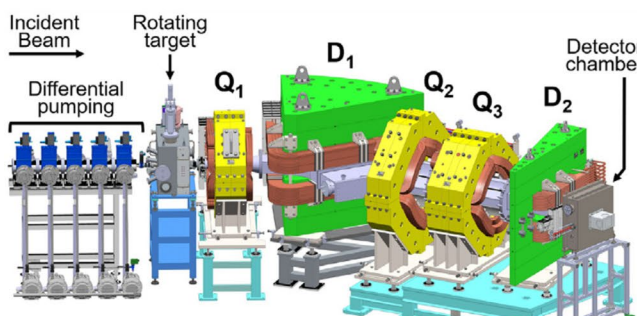


Fig. 5 (Color online) Schematic view (left) and photo (right) of SHANS2. Reproduced from Ref. [130]

resources and are limited by the accuracy of the interaction models.

TDHF theory can be derived from the time-dependent variational principle [162]. In the TDHF, the many-body wave function is approximated as a Slater determinant, automatically ensuring the Pauli exclusion principle. The TDHF method is a fully microscopic, parameter-free theory that unifies the nuclear structure and reactions within a single framework. Dynamic and quantum effects are automatically incorporated into this approach [163].

By constraining the density distribution obtained from the dynamical evolution in the TDHF method, the density-constrained time-dependent Hartree-Fock (DC-TDHF) model can be derived, allowing for the extraction of nucleus-nucleus potentials in heavy ion reactions. Using this method, Ref. [164] investigated the feasibility of forming a compound nucleus with $Z = 119$ via the $^{50}\text{Ti} + ^{249}\text{Bk}$ reaction.

The TDHF model can also be combined with phenomenological models to obtain more accurate predictions. In Ref. [165], the isotopic dependence of quasi-fission and fusion-fission in the production of flerovium isotopes was investigated. The TDHF method was applied for fusion and quasi-fission dynamics, while the statistical evaporation model HIVAP was used for fusion-fission dynamics. Reference [134] examined the orientation effects of the $^{48}\text{Ca} + ^{238}\text{U}$ reaction with the reaction dynamics described by

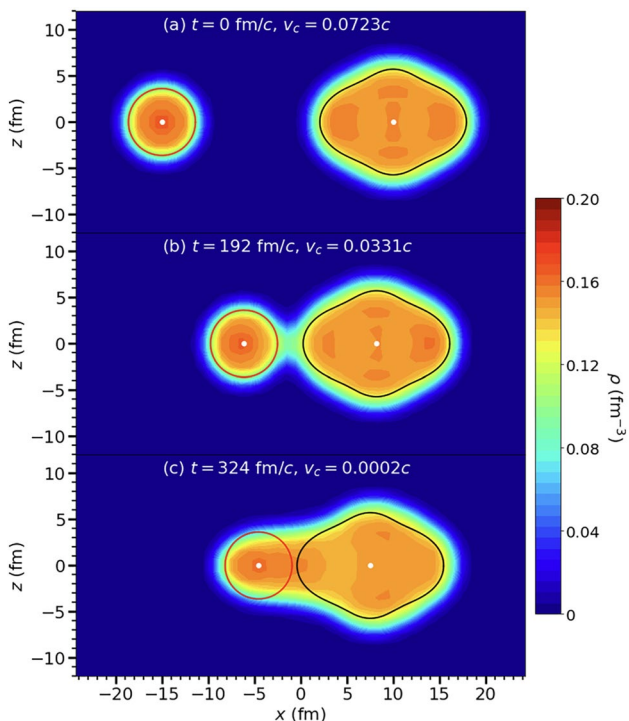


Fig. 6 (Color online) Time evolution of the density density of fusion reaction $^{48}\text{Ca} + ^{238}\text{U}$ with ^{238}U being tip orientation within the framework of TDHF model. Reproduced from Ref. [134]

TDHF theory, as illustrated in Fig. 6. This study combines the TDHF model with coupled-channel and FBD models, and predicts that the tip orientation is more favorable for both the capture process and formation of the compound nucleus in this reaction. Additionally, Ref. [137] combined the TDHF method with the Langevin equation, suggesting that differences in the probabilities of evaporation residue formation among reaction systems primarily originate from the evaporation process, which is sensitive to the fission barrier height and excitation energy of the compound nucleus.

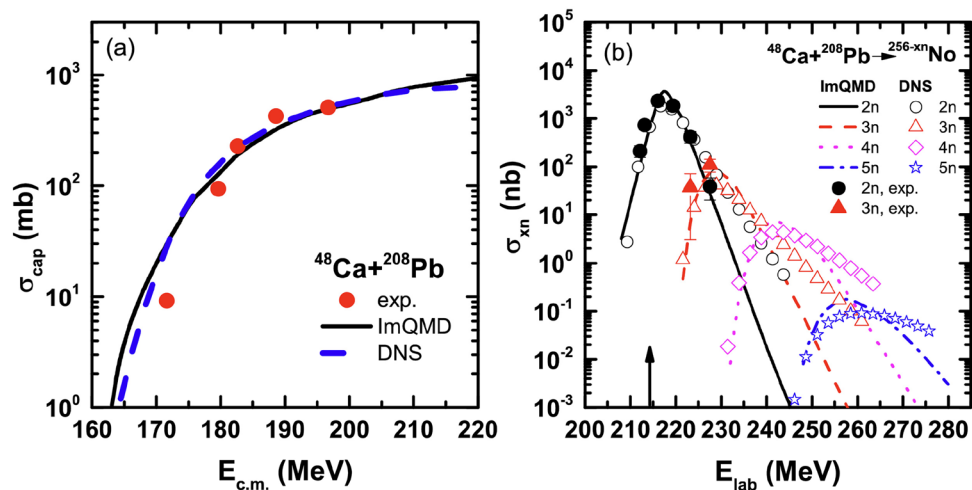
The QMD model is a microscopic model derived from the classical molecular dynamics (CMD) model and the many-body Schrödinger equation [166]. In the QMD model, each nucleon is represented by a Gaussian wave packet, incorporating both mean-field effects and two-body collisions [167]. Advanced variations of the QMD model, such as the isospin-dependent quantum molecular dynamics (IQMD) model and the improved quantum molecular dynamics (ImQMD) model, are particularly effective in describing the processes of low-energy heavy ion collisions.

Within the QMD model framework, the fusion process is considered to occur when two independent nuclei successfully overcome the Coulomb barrier and maintain a stable monomer density during rotation or oscillation of the compound nucleus. By simulating a large number of events, the fusion cross section at a specific incident energy can be statistically determined. In Ref. [131], the excitation functions predicted by the ImQMD model for the reaction $^{48}\text{Ca} + ^{208}\text{Pu}$ were compared with the results obtained from the DNS model and experimental data, as depicted in Fig. 7. This work confirmed the reliability of the ImQMD model and predicted the optimal projectile-target combinations for synthesizing $^{243-248}\text{No}$ isotopes. Additionally, Ref. [133] applied the IQMD model to investigate the enhanced fusion probabilities in reactions with ^{44}Ca beams, attributing the enhancement to the rapid development of the neck region and the higher neutron-to-proton ratio. The study also predicted the optimal projectile-target combinations for producing new $^{245-250}\text{Lr}$ isotopes, along with the corresponding incident energies.

4.2 Phenomenological models

In phenomenological models, dynamical evolution equations are established by incorporating certain collective degrees of freedom to describe the dynamics of nuclear reactions. These approaches simplify the computational process by neglecting the intricate interactions among the nucleons. With the de-excitation process treated using statistical models, the HIVAP code, the KEWPIE code or the GEMINI++ model [143, 168–171], phenomenological models can be effectively applied to heavy ion collision reactions near the Coulomb barrier.

Fig. 7 (Color online) The experimental and calculated capture and ER cross sections of the $^{48}\text{Ca} + ^{208}\text{Pb}$ reaction. Reproduced from Ref. [131]



One approach for describing the fusion process considers the dynamic evolution of the formed mononucleus, proposing that once the projectile and target nuclei come into contact, they rapidly lose their individuality and form a highly deformed nucleus. Fusion is considered to occur when the deformed nucleus gradually evolves into a spherical compound nucleus; otherwise, quasi-fission occurs. The macroscopic dynamical model was the first to describe the fusion mechanism based on this concept [172–175]. In this model, the nucleus is treated as a viscous liquid drop, and the fusion process is regarded as a purely dynamic phenomenon that can be described using

classical equations of motion. However, this model faced challenges in reproducing the ER cross sections for fusion reactions, as it did not account for the competition between fusion and quasi-fission, nor did it incorporate the shell effect [176]. To address these limitations, the two-step model [143–145, 177] and fusion-by-diffusion model [139, 140] introduced shell effects in the calculation of the potential energy surface, along with statistical fluctuations in the interaction of colliding nuclei [178]. These enhancements have allowed for more accurate reproduction and prediction of ER cross sections in fusion reactions.

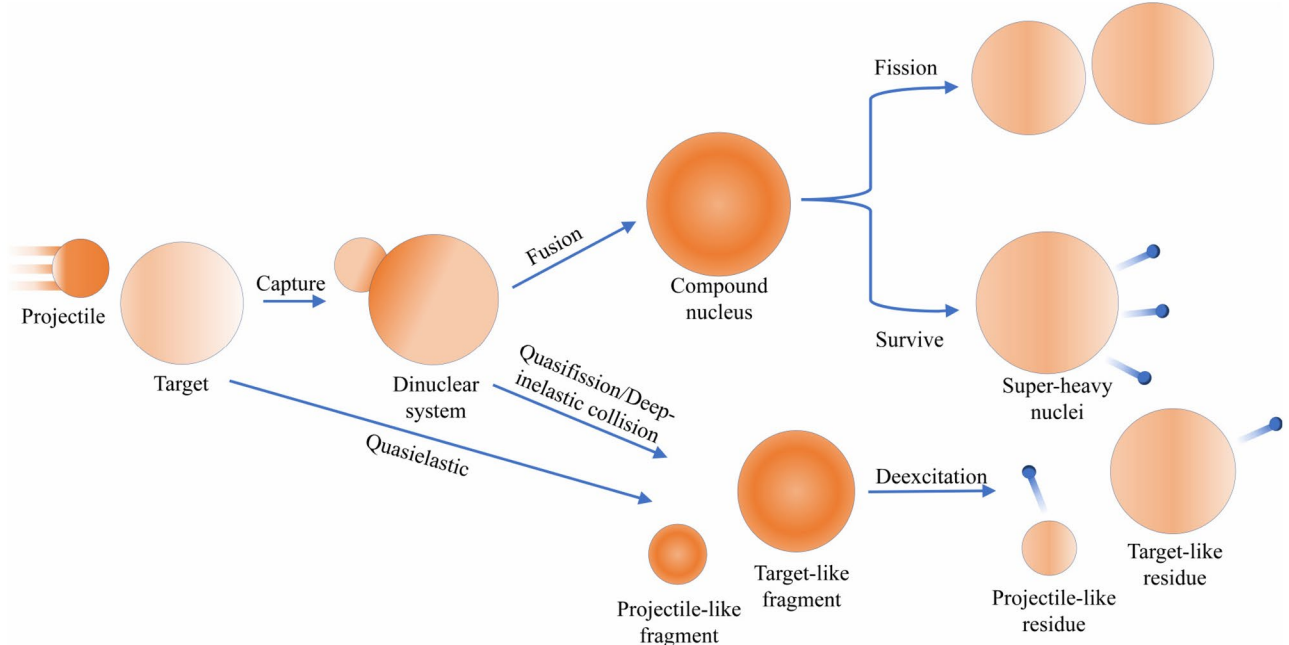


Fig. 8 (Color online) Schematic illustration of heavy ion collisions within the DNS model framework. Reproduced from Ref. [179]

Another description of the fusion process focuses on the degree of freedom of the mass asymmetry. In these models, the two nuclei retain their individuality and nucleon transfer occurs within the formed dinuclear system, as depicted in Fig. 8. Fusion is considered to occur when all the nucleons from the projectile are successfully transferred to the target nucleus. Conversely, quasi-fission process takes place when nucleons are transferred from the target nucleus to the projectile [179].

Based on this assumption, the DNS model was developed. The nucleon transfer process within the DNS model is treated by solving a set of master equations, which are governed by the potential energy surface considering nuclear structure effects [154]. The calculated results for cold and hot fusion reactions using the dinuclear system model match well with available experimental data [157, 180]. However, this approach initially did not consider the dynamic factors influencing the fusion stage. To address this, Ref. [153] coupled the dynamic deformation of the nucleus with nucleon transfer within the DNS model, and predicted the ER cross sections for the synthesis of a new SHE. In recent years, neural networks and machine learning methods have been introduced to optimize nuclear data and refine the parameters of the theoretical model [181–184].

The nucleon collectivization model offers an intermediate approach for describing the fusion process compared with the previously mentioned methods [185]. In this model, within the formed dinuclear system, a portion of nucleons is considered to become “common” nucleon, shared by both nuclei. Fusion is thought to occur when all nucleons are transformed into common nucleons; otherwise, quasi-fission occurs. Although this model successfully describes the excitation function of hot fusion reactions, the physical concept of the introduced common nucleons remains highly controversial.

Given the significant difference in the descriptions of the fusion process across various models, some researchers have attempted to combine fusion mechanisms from different theoretical models and experimental observations to develop relatively simple empirical formulas for calculating fusion probability [186–191]. These formulas, informed by

experimental phenomena and theoretical approaches, identify several influential factors in the fusion process, including the excitation energy, quasi-fission barrier, compound nucleus mass or charge number, and mass asymmetry [186, 188, 189]. These empirical formulas effectively reproduce the experimental results of the known fusion reactions. Recently, a model-independent method, based on the Coulomb barrier height of side-side collisions and Q value, was established to predict the optimal incident energies for unknown reaction systems [192]. This approach allows the estimation of optimal incident energies with minimal uncertainty.

5 Efforts in the Synthesis of New Superheavy Elements with $Z = 119, 120$

Since the synthesis of Oganesson through the reaction $^{48}\text{Ca} + ^{249}\text{Cf} \rightarrow ^{294}\text{Og} + 3\text{n}$, the seventh period of the periodic table was completed. However, for the synthesis of SHE with atomic numbers $Z > 118$, the ^{48}Ca -induced fusion reactions are restricted by the limited availability of Einsteinium and Fermium targets. Consequently, heavier beams, such as ^{50}Ti , ^{51}V , and ^{54}Cr , must be applied.

The experimental attempts to synthesize a new SHE are summarized in Table 2. Initially, GSI attempted to synthesize the SHE with $Z = 120$ using the reaction $^{64}\text{Ni} + ^{238}\text{U}$ in 2008 [193], and JINR attempted the reaction $^{58}\text{Fe} + ^{244}\text{Pu}$ in 2009 [194]. However, no corresponding α decay chains were observed in these experiments. In 2016, GSI attempted to synthesize element with $Z = 120$ via the reaction $^{54}\text{Cr} + ^{248}\text{Cm}$ [195, 196], observing three α decay chains attributed to $^{299}120$. Unfortunately, these were later identified as random events [197]. Additionally, in 2020, GSI conducted experiments to search for the new elements with $Z = 119$ and $Z = 120$ using the reactions $^{50}\text{Ti} + ^{249}\text{Bk}$ and $^{50}\text{Ti} + ^{249}\text{Cf}$, respectively, but no evidence of a new SHE was found [198]. In 2022, RIKEN investigated the quasielastic barrier distribution for the reaction $^{51}\text{V} + ^{248}\text{Cm}$ and deduced the optimal reaction energy for synthesizing element with $Z = 119$ through this reaction [199].

Table 2 The experimental progress of the synthesis of SHEs with $Z > 118$

Element	Year	Laboratory	Reaction	Results	Detection limit	Ref.
$Z = 120$	2008	GSI	$^{64}\text{Ni} + ^{238}\text{U}$	No observed α decay chain	0.09 pb	[193]
$Z = 120$	2009	JINR	$^{58}\text{Fe} + ^{244}\text{Pu}$	No observed α decay chain	0.4 pb	[194]
$Z = 120$	2016	GSI	$^{54}\text{Cr} + ^{248}\text{Cm}$	Three observed random α decay chains	0.58 pb	[195]
$Z = 119$	2020	GSI	$^{50}\text{Ti} + ^{249}\text{Bk}$	No observed α decay chain	0.065 pb	[198]
$Z = 120$	2020	GSI	$^{50}\text{Ti} + ^{249}\text{Cf}$	No observed α decay chain	0.2 pb	[198]
$Z = 119$	2022	RIKEN	$^{51}\text{V} + ^{248}\text{Cm}$	Optimal reaction energy estimated		[199]

In 2024, the reaction $^{50}\text{Ti} + ^{244}\text{Pu}$ was investigated at the LBNL 88-Inch Cyclotron Facility, producing an isotope ^{290}Lv with an ER cross section of 0.44 pb [200]. Although the ER cross section is lower than that of the ^{48}Ca -induced reactions, this experiment proves the feasibility of using a ^{50}Ti beam for the production of a new SHE [201]. Recently, the upgraded experimental facility HIFRL-CAFE2 was tested using the reaction $^{48}\text{Ca} + ^{243}\text{Am}$. The synthesis of the element with $Z = 119$ via the reaction $^{54}\text{Cr} + ^{243}\text{Am}$ is currently underway. JINR has also planned to explore the reactions $^{50}\text{Ti} + ^{249}\text{Bk}$ and $^{54}\text{Cr} + ^{243}\text{Am}$ for synthesizing the 119th element, as well as the reactions $^{50}\text{Ti} + ^{249}\text{Cf}$ and $^{54}\text{Cr} + ^{248}\text{Cm}$ for the 120th element [202]. The nuclei to be searched are summarized in Fig. 9.

Various theoretical models have predicted the optimal projectile-target combinations and corresponding incident energies for new elements beyond Oganesson via fusion reactions [140, 142, 143, 153, 157, 188, 189, 203–210]. Figure 10 shows the optimal reaction energies predicted in Ref. [157] and estimated by RIKEN for the reaction $^{51}\text{V} + ^{248}\text{Cm}$, with a strong agreement between the predicted and estimated energies. As summarized in Ref. [157] and Ref. [200], most models identify the reactions $^{50}\text{Ti} + ^{249}\text{Bk}$ and $^{50}\text{Ti} + ^{249}\text{Cf}$ as advantageous for producing SHE with $Z = 119$ and $Z = 120$. The predicted maximal ER cross sections from different models generally fall within the feto-barn range, although the optimal incident energies can differ by several MeV for certain reactions. Additionally, based on measurements of the mass and angular distributions of fission fragments, Ref. [211] also predicted that the reaction $^{50}\text{Ti} + ^{249}\text{Cf}$ shows promise for synthesizing SHE with $Z = 120$. For the synthesis of SHE with $Z = 121$, Ref. [156] suggested that the reactions $^{46}\text{Ti} + ^{252}\text{Es}$ and $^{46}\text{Ti} + ^{254}\text{Es}$ could be feasible in future experiments, with maximal ER cross sections expected to reach several fetobarns.

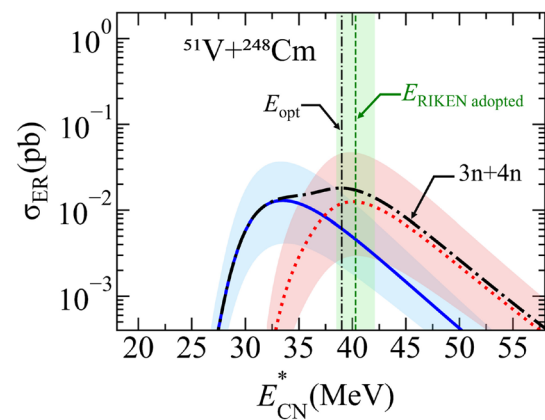


Fig. 10 (Color online) Comparison of the optimal reaction energy predicted by DNS model and estimated by RIKEN [199] for the reaction $^{51}\text{V} + ^{248}\text{Cm}$. Reproduced from Ref. [157]

Recently, researchers proposed high-energy alpha particle emission as a novel mechanism for synthesizing new elements [212]. In the experiments conducted at JINR, the energy spectra of α particles emitted from the reactions $^{40}\text{Ar} + ^{232}\text{Th}$ and $^{48}\text{Ca} + ^{238}\text{U}$ at near-barrier energies were measured. The results indicated that at the kinematic limit, the observed cross sections were in the picobarn range. These experiments revealed that two-body reactions facilitate the production of heavy residue nuclei with minimal excitation energy, thereby enhancing their survival probability. Consequently, this reaction mechanism can potentially produce SHN with ER cross sections that are several orders of magnitude greater than those achieved through traditional fusion-evaporation reactions.

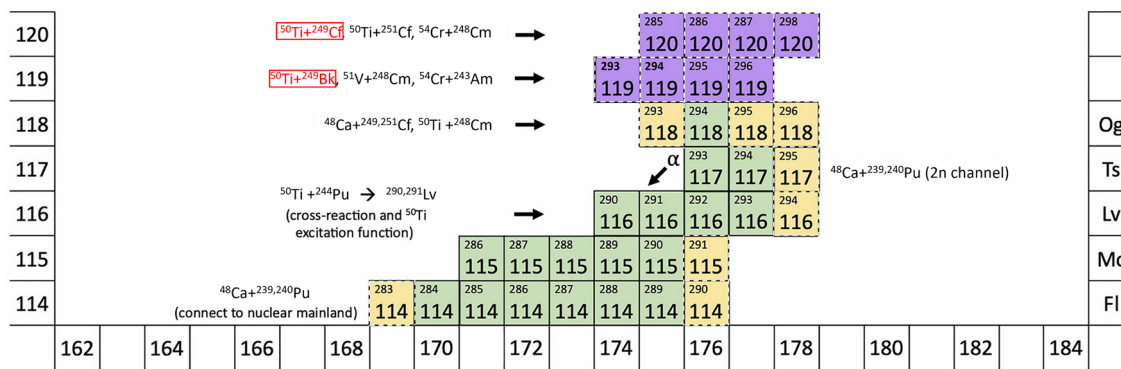


Fig. 9 (Color online) SHN region with $Z \geq 114$. Green, purple and yellow colors represent the synthesized SHNs, SHNs planned to be searched and SHNs with a clear path to discovery. The theoretically

predicted most feasible reactions for synthesizing elements with $Z = 119$ and 120 are marked with red boxes. Reproduced from Ref. [202]

6 Current Challenges and Future Directions

The synthesis of new SHNs faces several challenges, including short half-lives and high instability of both the target materials and the produced nuclei [213, 214]. The maximal ER cross sections in the hot fusion reactions also approached the detection limit. Moreover, the limited availability of actinide targets requires the use of heavier projectiles in future experiments [200], which is expected to further suppress ER cross sections compared to those induced by ^{48}Ca . To address these challenges, nuclear physics laboratories worldwide are upgrading their equipment, as discussed in Sect. 3, to achieve higher beam intensities and enhanced detection precision.

In various theoretical models, many assumptions and approximations have been adopted, such as employing the double-folding potential with a sudden approximation to calculate the nuclear potential, assuming quadrupole or hexadecapole deformations of the nucleus, and using empirical surface diffusion coefficients. The fission barrier in the de-excitation process is typically described in one-dimensional parameterized form. Precise nuclear masses of superheavy nuclei are also crucial [215–217]. As demonstrated in Refs. [218, 219], even predictions made using the same model can vary significantly when based on different mass tables.

Although these assumptions and approximations are necessary because of the current limitations in computational resources and theoretical development, the uncertainties introduced by empirical parameters and approximations constrain the extrapolative capability of the models and cannot be ignored. Some studies have attempted to estimate the uncertainties originating from these empirical parameters or to constrain them using microscopic approaches [146, 157, 158, 220]. However, a comprehensive evaluation of the uncertainties introduced by these empirical methods is required.

Calculations in the SHN region using microscopic models involve handling the interactions among a large number of nucleons, often resulting in computation times ranging from several months to years. This limitation significantly restricts the application of microscopic models in SHE research. While advancements in computational power, as predicted by Moore's law, may alleviate this issue, the introduction of new parallel computing methods presents a more immediate solution. Researchers are exploring ways to identify the key physical degrees of freedom in nuclear reactions to develop new phenomenological models. Additionally, the limited amount of experimental data from ^{48}Ca -induced reactions hinders the verification of theoretical models, raising concerns regarding their reliability when extrapolating to reactions involving heavier projectiles. More experimental

data from a variety of projectile-target combinations are also needed to develop more robust theoretical models.

Currently, α decay tagging is the primary technique for identifying reaction products, but it is limited by the requirement that synthesized nuclei have suitable half-lives and unambiguous decay chains. As a result, many SHNs in the neutron-rich region cannot be identified using this method. Therefore, new identification techniques, such as high-precision mass measurements, laser resonance ionization, and a combination of mass separation with decay tagging, should be considered [221–223].

The relatively low neutron-to-proton ratio in both the projectile and target nuclei during the fusion reactions leads to the formation of a compound nucleus with a reduced neutron number. Additionally, the compound nucleus must undergo neutron evaporation to reach its ground state, resulting in the production of nuclei that are typically neutron-deficient. Such conditions present a significant challenge for the production of neutron-rich superheavy nuclei, as the heaviest available targets are currently ^{249}Cf and ^{249}Bk .

The actinide target nuclei used in fusion reactions are produced through the intense neutron irradiation of targets composed of mixed Pu, Am, and Cm in high-flux reactors, as illustrated in Fig. 11. Currently, reactors capable of providing these actinide materials include the High Flux Isotope Reactor (HFIR) at the Oak Ridge National Laboratory [224], the Advanced Test Reactor (ATR) at Idaho National Laboratory [225], and the SM-3 Reactor at the Research Institute of Advanced Reactors (RIAR) in Dimitrovgrad [226]. Additionally, the Jules Horowitz Reactor (JHR) [227] and the Tsinghua High Flux Reactor (THFR) [228], which are currently under construction, will also provide heavy actinide targets. In future experiments, new actinide target materials, particularly neutron-rich targets, such as ^{251}Cf and ^{254}Es , could be produced and applied in fusion reactions [202].

Theoretical studies suggest an “island of stability” where enhanced shell effects lead to long-lived nuclei. However, the precise location of this area remains uncertain because of the varying predictions from different nuclear models. Macroscopic-microscopic models employing different potentials, such as Nilsson, Woods-Saxon, and folded Yukawa, typically locate the center at $Z = 114$, $Z = 184$ [11, 12, 229, 230]. Depending on the selected parameters, self-consistent models using Skyrme-Hartree-Fock or relativistic mean field interactions predict various combinations of $Z = 114$, 120, 124, or 126, and $Z = 172$ or 184 [14, 15, 15–20]. In recent years, researchers have been investigating novel reaction mechanisms to explore the neutron-rich superheavy region and reach the center of the “island of stability”. Radioactive beam-induced fusion reactions have been proposed as methods for synthesizing neutron-rich SHN [159, 190, 222, 231, 232]. Additionally, multi-nucleon transfer (MNT) reactions

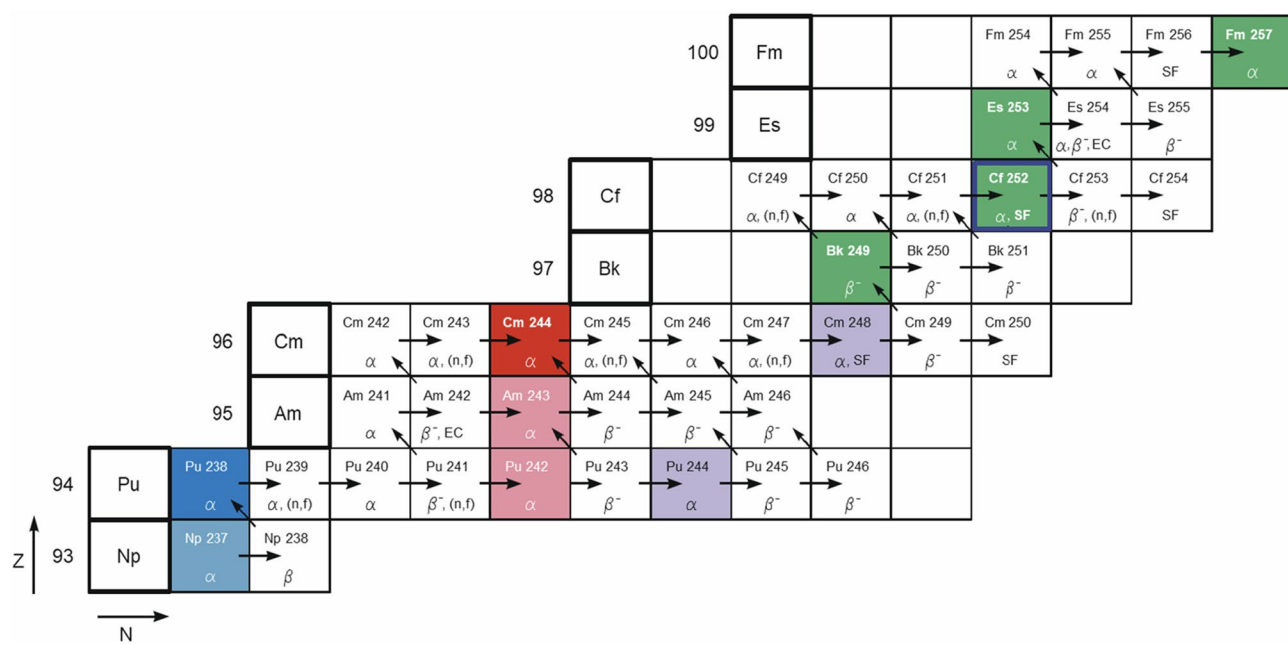


Fig. 11 (Color online) Reactor production of transcurium actinides from multiple neutron captures and beta decays. The light-colored squares represent the target isotopes irradiated under ORNL's Pluto-

nium-238 Supply Program and Californium-252 Program. The dark-colored squares represent the heavy actinide target isotopes that can be produced. Reproduced from Ref. [202]

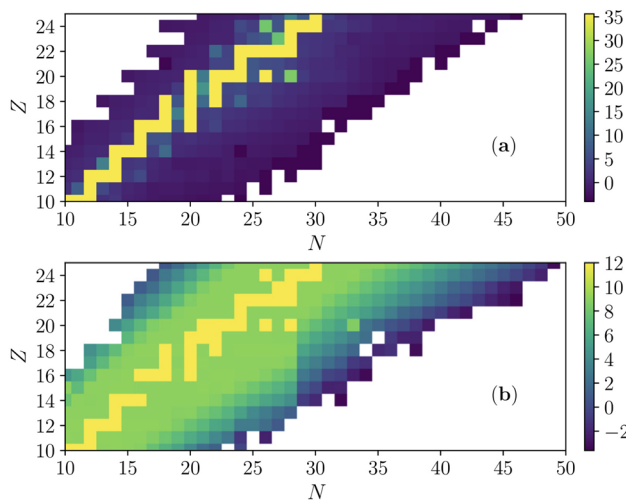


Fig. 12 (Color online) **a** The \log_{10} value of the half-lives (s) and **b** of the beam intensities (p/s) for the nuclei with $10 \leq Z \leq 25$. Reproduced from Ref. [159]

have been suggested as promising approaches for producing neutron-rich isotopes [1–3, 222, 232–238].

6.1 Radioactive beams

Compared to stable beams, neutron-rich radioactive projectiles have higher neutron-to-proton ratios, enabling exploration of the neutron-rich SHN region. Figure 12 summarizes

the possible radioactive beams that can be generated at the Argonne Tandem Linac Accelerator System (ATLAS). However, a significant challenge for radioactive beam-induced fusion reactions is low beam intensity. Although stable beam intensities can reach the order of 10^{12} p/s, the intensities of radioactive beams are currently much weaker. To address this limitation, modern radioactive beam accelerator facilities, such as the Radioactive Isotope Beam Factory (RIBF) and the Second-generation System On-Line Production of Radioactive Ions (Spiral2) [239, 240], are working on upgrading their capabilities to achieve high-intensity exotic ion beams [222, 241].

Many theoretical studies have investigated the mechanisms of radioactive beam-induced fusion reactions. Reference [242] predicted that the reaction induced by the neutron-rich radioactive beam ^{46}Ar could produce new neutron-rich nuclei $^{290-292}\text{Fl}$, provided that the beam intensity was sufficient. Reference [159] explored the production of neutron-rich SHN with $Z = 105-118$ through radioactive beam-induced fusion reactions. Additionally, Ref. [243] examined the possibility of reaching the “island of stability” via radioactive beams and ^{244}Pu , ^{248}Cm , ^{249}Cf targets.

6.2 Multi-nucleon transfer reactions

Several MNT reaction experiments have been conducted in recent years. In 2018, significant α particle emission was observed in the reaction $^{238}\text{U} + ^{232}\text{Th}$ [244]. A comparison

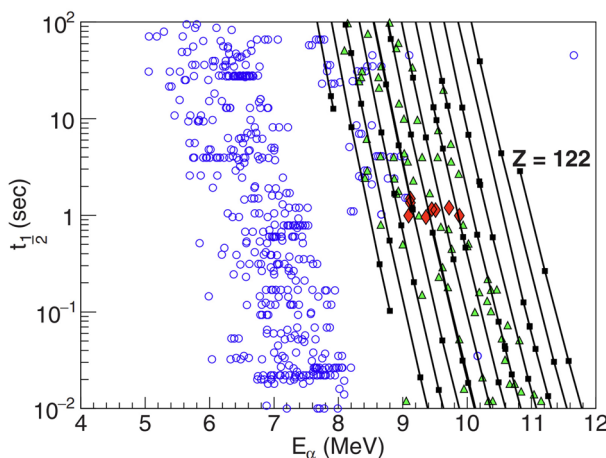


Fig. 13 (Color online) The measured α particle energy and half-life in the $^{238}\text{U} + ^{232}\text{Th}$ experiment (diamonds). Previous experimental results are indicated by the circles and triangles, the theoretical predictions are denoted by the squares. Reproduced from Ref. [244]

between the experimental results and theoretical calculations suggested the possible formation of unknown neutron-rich nuclei with atomic numbers of up to 116, as depicted in Fig. 13. However, owing to limitations in the detection methods, the cross section information for these formed nuclei was not measured. Significant advancement in the production of new nuclei via MNT reactions was achieved in 2015 at the UNILAC accelerator at GSI, where the reaction $^{48}\text{Ca} + ^{248}\text{Cm}$ was studied. This experiment resulted in the identification of five new neutron-deficient isotopes: ^{216}U , ^{219}Np , ^{223}Am , ^{229}Am and ^{233}Bk [245]. These findings demonstrate that the MNT reactions can be effectively utilized to synthesize neutron-deficient transuranium nuclei. In 2023, RIKEN discovered a new neutron-rich nucleus, ^{241}U , through the MNT reaction $^{238}\text{U} + ^{198}\text{Pt}$, demonstrating the feasibility of MNT reactions for producing neutron-rich nuclei near the $N = 152$ subshell [246].

Several theoretical models, such as the DNS model [6, 247–251], GRAZING model [252–254], QMD model [252, 255, 256], Langevin equations [257, 258], time-dependent covariant density functional theory [259], and TDHF model [256, 260–264] have also been applied to investigate MNT reactions. In Ref. [265], the reliability of DNS model in MNT reactions was validated, predicting the production cross sections of four new Rf isotopes through the $^{238}\text{U} + ^{252}\text{Cf}$ reaction. Reference [266] combined the GRAZING model framework with the DNS model, significantly enhancing the theoretical descriptions of experimental results for MNT reactions. Reference [267] introduced the deformation degree of freedom and Monte Carlo de-excitation methods, leading to the development of an improved DNS-sysu model, and explored the feasibility of reaching the “island of stability” through

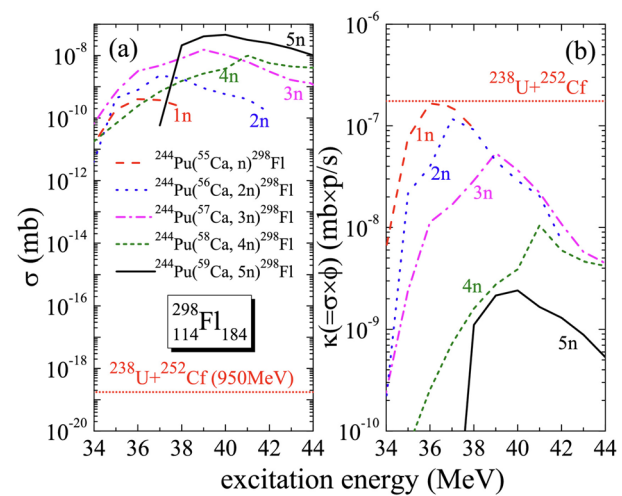


Fig. 14 (Color online) Comparison of the production cross sections and cross-section \times beam intensity factors for producing the predicted double magic nucleus ^{298}Fl via the radioactive beam-induced and MNT reactions. Reproduced from Ref. [267]

radioactive beam-induced fusion reactions and MNT reactions, as shown in Fig. 14.

Based on the ImQMD model, Ref. [268] studied the production cross sections of superheavy isotopes formed in the $^{238}\text{U} + ^{238}\text{U}$ reaction, finding that the isospin dependence of the fission barrier results in production cross sections for neutron-rich isotopes 254 – ^{256}Cf being nearly three orders of magnitude lower than those of ^{249}Cf . Reference [252] presents a comparison of the mass distributions of primary binary fragments predicted by the ImQMD, DNS, and GRAZING models with experimental data, as shown

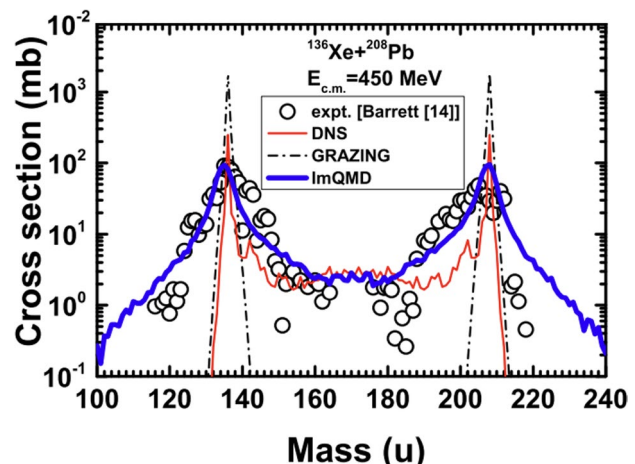


Fig. 15 (Color online) Mass distributions of primary binary fragments calculated with the ImQMD (thick solid line), DNS (thin solid line), and GRAZING (dash-dot line) model. The experimental data taken from Ref. [254] is represented by the open circles. Reproduced from Ref. [252]

in Fig. 15. The study reveals that the DNS and GRAZING models are primarily suitable for describing transfer processes involving only a few nucleons between the projectile and target. In contrast, the ImQMD model shows a high level of agreement with experimental results across most mass regions.

For the TDHF model, Ref. [262] observed that in the $^{238}\text{U} + ^{124}\text{Sn}$ reaction, owing to the inverse quasi-fission process, ^{124}Sn can transfer a large number of nucleons to ^{238}U , leading to the formation of new isotopes. By employing a multidimensional dynamical model based on Langevin equations, Ref. [269] explored the production of heavy transuranium nuclei during collisions with actinide nuclei. The results suggest the feasibility of synthesizing several neutron-rich heavy actinide isotopes, with production cross sections surpassing 1 μb . Additionally, new methods based on the master and Langevin equations have been applied to MNT reactions [270, 271]. The feasibility of MNT reactions with radioactive beams has been investigated in several studies [272–275].

7 Summary

The search for new superheavy nuclei achieved significant success, particularly with the completion of the seventh period of the periodic table. Despite these accomplishments, the synthesis of elements beyond $Z = 118$ remains a substantial challenge, largely because of the limited availability of actinide targets and rapidly decreasing ER cross sections. Employing heavier projectiles is a promising approach for the synthesis of new superheavy elements. The feasibility of the ^{50}Ti projectile is experimentally validated. The investigation of new reaction mechanisms, including radioactive beam-induced fusion reactions and multi-nucleon transfer reactions, presents promising pathways for producing neutron-rich superheavy nuclei and for approaching the next shell closure. Recent developments in theoretical models have provided valuable predictions for optimizing experimental conditions. However, the reliability of these models requires further validation. Continued upgrades to accelerator beam intensities and detector efficiencies, coupled with the development of more precise theoretical models, will be crucial for overcoming the challenges associated with the synthesis of new superheavy elements.

Acknowledgements We warmly thank Prof. Wenqing Shen for the encouragement on heavy ion physics over a long period of time. F. S. Zhang and the other authors thank Y. Abe, D. Ackermann, G. G. Adamian, R. An, N. V. Antonenko, S. Ayik, X. J. Bao, D. Boilley, L. G. Cao, L. W. Chen, M. Colonna, L. R. Dai, D. Q. Fang, L. S. Geng, C. C. Guo, B. Guo, L. Guo, S. Heinz, H. Hua, D. A. Ibadullayev, A. V. Karpov, E. Kozulin, B. A. Li, C. Li, J. J. Li, M. Liu, Q. F. Li, C. J. Lin, H. N. Liu, W. P. Liu, Z. Liu, W. Loveland, C. W. Ma, Y. G. Ma,

J. Meng, J. Natowitz, A. K. Nasirov, Y. T. Oganessian, J. C. Pei, M. Płoszajczak, Z. Z. Ren, A. Rodin, V. V. Sargsyan, C. W. Shen, W. Q. Shen, M. Shumeiko, B. H. Sun, Z. Y. Sun, A. Svirikhin, J. Su, J. Tang, X. D. Tang, B. Tsang, Y. S. Tsyganov, V. K. Utyonkov, M. Veselsky, A. A. Voinov, J. S. Wang, M. Wang, N. Wang, P. W. Wen, G. Q. Xiao, Z. G. Xiao, C. X. Yuan, C. Y. Wong, F. R. Xu, H. S. Xu, J. C. Yang, A. V. Yeremin, W. Ye, Y. L. Ye, W. L. Zhan, G. Zhang, H. F. Zhang, H. Q. Zhang, S. S. Zhang, X. R. Zhang, Y. H. Zhang, Y. X. Zhang, E. G. Zhao, K. Zhao, Y. M. Zhao, X. H. Zhou, L. Zhu and Z. Y. Zhu for valuable discussions on the synthesis of superheavy nuclei.

References

1. Y.G. Ma, *Recent Progress in Nuclear Physics* (Shanghai Jiao Tong University Press, Shanghai, 2020)
2. D.Z. Ding, Y.S. Chen, H.Q. Zhang, *Progress in Nuclear Physics* (Shanghai Scientific and Technological Publishing House, Shanghai, 1997)
3. F.S. Zhang, L.X. Ge, *Nuclear Multifragmentation* (Science Press, Beijing, 1998)
4. E. McMillan, P.H. Abelson, *Radioactive Element 93*. Phys. Rev. **57**, 1185–1186 (1940). <https://doi.org/10.1103/PhysRev.57.1185.2>
5. M. Thoennessen, *The Discovery of Isotopes* (Springer, Switzerland (2016). <https://doi.org/10.1007/978-3-319-31763-2>
6. F.S. Zhang, C. Li, L. Zhu et al., Production cross sections for exotic nuclei with multinucleon transfer reactions. *Front. Phys.* **13**(6), 132113 (2018). <https://doi.org/10.1007/s11467-018-0843-6>
7. F.S. Zhang, Z.Y. Ming, G.M. Jin, Progress of synthesis of superheavy nuclei. *Prog. Phys.* **21**(1), 29–44 (2001)
8. S.G. Zhou, Superheavy nuclei and superheavy elements. *Physics* **43**(12), 817–825 (2014). <https://doi.org/10.7693/wl20141206>
9. L.L. Li, B.N. Lv, N. Wang et al., Theoretical study of structure and synthesis mechanism of superheavy nuclei. *Nucl. Phys. Rev.* **31**(3), 253–272 (2014). <https://doi.org/10.11804/NuclPhysRev.31.03.253>
10. S.G. Zhou, Study on superheavy nuclei and superheavy elements. *Nucl. Phys. Rev.* **34**(3), 318–331 (2017). <https://doi.org/10.11804/NuclPhysRev.34.03.318>
11. A. Sobiczewski, F.A. Gareev, B.N. Kalinkin, Closed shells for $Z > 82$ and $N > 126$ in a diffuse potential well. *Phys. Lett.* **22**(4), 500–502 (1966). [https://doi.org/10.1016/0031-9163\(66\)91243-1](https://doi.org/10.1016/0031-9163(66)91243-1)
12. H. Meldner, *Arkiv Fysik* **36**, 593 (1967)
13. P. Möller, A.J. Sierk, T. Ichikawa et al., Nuclear ground-state masses and deformations: FRDM(2012). *At. Data Nucl. Data Tables* **109–110**, 1–204 (2016). <https://doi.org/10.1016/j.adt.2015.10.002>
14. S. Ćwiok, J. Dobaczewski, P.H. Heenen et al., Shell structure of the superheavy elements. *Nucl. Phys. A* **611**(2), 211–246 (1996). [https://doi.org/10.1016/S0375-9474\(96\)00337-5](https://doi.org/10.1016/S0375-9474(96)00337-5)
15. S. Ćwiok, P.H. Heenen, W. Nazarewicz, Shape coexistence and triaxiality in the superheavy nuclei. *Nature* **433**, 705–709 (2005). <https://doi.org/10.1038/nature03336>
16. D. Ackermann, C. Theisen, Nuclear structure features of very heavy and superheavy nuclei—tracing quantum mechanics towards the ‘island of stability’. *Phys. Scr.* **92**(8), 083002 (2017). <https://doi.org/10.1088/1402-4896/aa7921>
17. K. Rutz, M. Bender, T. Bürvenich et al., Superheavy nuclei in self-consistent nuclear calculations. *Phys. Rev. C* **56**, 238–243 (1997). <https://doi.org/10.1103/PhysRevC.56.238>

18. A.T. Kruppa, M. Bender, W. Nazarewicz et al., Shell corrections of superheavy nuclei in self-consistent calculations. *Phys. Rev. C* **61**, 034313 (2000). <https://doi.org/10.1103/PhysRevC.61.034313>
19. A. Sobiczewski, K. Pomorski, Description of structure and properties of superheavy nuclei. *Prog. Part. Nucl. Phys.* **58**(1), 292–349 (2007). <https://doi.org/10.1016/j.ppnp.2006.05.001>
20. M. Ismail, A.Y. Ellithi, A. Adel et al., On magic numbers for super- and ultraheavy systems and hypothetical spherical double-magic nuclei. *J. Phys. G Nucl. Part. Phys.* **43**(1), 015101 (2015). <https://doi.org/10.1088/0954-3899/43/1/015101>
21. O.R. Smits, C.E. Düllmann, P. Indelicato et al., The quest for superheavy elements and the limit of the periodic table. *Nat. Rev. Phys.* **6**, 86–98 (2024). <https://doi.org/10.1038/s42254-023-00668-y>
22. A. Ghiroso, M. Nurmia, J. Harris et al., Positive identification of two alpha-particle-emitting isotopes of element 104. *Phys. Rev. Lett.* **22**, 1317–1320 (1969). <https://doi.org/10.1103/PhysRevLett.22.1317>
23. A. Ghiroso, M. Nurmia, K. Eskola et al., ^{261}Rf ; new isotope of element 104. *Phys. Lett. B* **32**(2), 95–98 (1970). [https://doi.org/10.1016/0370-2693\(70\)90595-2](https://doi.org/10.1016/0370-2693(70)90595-2)
24. K. Eskola, P. Eskola, M. Nurmia et al., Studies of lawrencium isotopes with mass numbers 255 through 260. *Phys. Rev. C* **4**, 632–642 (1971). <https://doi.org/10.1103/PhysRevC.4.632>
25. R.C. Barber, N.N. Greenwood, A.Z. Hrynkiewicz et al., Discovery of the transfermium elements. Part ii: Introduction to discovery profiles. Part iii: Discovery profiles of the trans-fermium elements (note: For part I see *Pure Appl. Chem.*, vol. 63, no. 6, pp. 879–886, 1991). *Pure and Appl. Chem.* **65** (8), 1757–1814 (1993). <https://doi.org/10.1351/pac199365081757>
26. G.N. Flerov, Y.T. Oganessian, Y.V. Lobanov et al., The synthesis of element 105. *Sov. At. Energy* **29**, 967–975 (1970)
27. K. Morita, K. Morimoto, D. Kaji et al., Experiment on the synthesis of element 113 in the reaction $^{209}\text{Bi}(^{70}\text{Zn}, \text{n})^{278}\text{113}$. *J. Phys. Soc. Jpn.* **73**, 2593 (2004). <https://doi.org/10.1143/jpsj.73.2593>
28. S. Hofmann, G. Münzenberg, The discovery of the heaviest elements. *Rev. Mod. Phys.* **72**, 733 (2000). <https://doi.org/10.1103/RevModPhys.72.733>
29. Y.T. Oganessian, V.K. Utyonkov, Y.V. Lobanov et al., Synthesis of the isotopes of elements 118 and 116 in the ^{249}Cf and $^{245}\text{Cm} + ^{48}\text{Ca}$ fusion reactions. *Phys. Rev. C* **74**, 044602 (2006). <https://doi.org/10.1103/PhysRevC.74.044602>
30. Y.T. Oganessian, A.V. Yeremin, A.G. Popeko et al., Synthesis of nuclei of the superheavy element 114 in reactions induced by ^{48}Ca . *Nature* **400**, 242 (1999). <https://doi.org/10.1038/22281>
31. Y.T. Oganessian, F.S. Abdullin, S.N. Dmitriev et al., Investigation of the $^{243}\text{Am} + ^{48}\text{Ca}$ reaction products previously observed in the experiments on elements 113, 115, and 117. *Phys. Rev. C* **87**, 014302 (2013). <https://doi.org/10.1103/PhysRevC.87.014302>
32. Y.T. Oganessian, V.K. Utyonkov, Y.V. Lobanov et al., Observation of the decay of $^{292}\text{116}$. *Phys. Rev. C* **63**, 011301(R) (2000). <https://doi.org/10.1103/PhysRevC.63.011301>
33. Y.T. Oganessian, F.S. Abdullin, P.D. Bailey et al., Synthesis of a new element with atomic number $Z = 117$. *Phys. Rev. Lett.* **104**, 142502 (2010). <https://doi.org/10.1103/PhysRevLett.104.142502>
34. <https://www.nndc.bnl.gov/nudat3/guide/>
35. L.P. Somerville, M.J. Nurmia, J.M. Nitschke et al., Spontaneous fission of rutherfordium isotopes. *Phys. Rev. C* **31**, 1801–1815 (1985). <https://doi.org/10.1103/PhysRevC.31.1801>
36. A. Ghiroso, M. Nurmia, K. Eskola et al., Two new alpha-particle emitting isotopes of element 105, ^{261}Ha and ^{262}Ha . *Phys. Rev. C* **4**, 1850–1855 (1971). <https://doi.org/10.1103/PhysRevC.4.1850>
37. Z.G. Gan, Z. Qin, H.M. Fan et al., A new alpha-particle-emitting isotope ^{259}Db . *Eur. Phys. J. A* **10**, 21–25 (2001). <https://doi.org/10.1007/s100500170140>
38. J. Dvorak, W. Brüchle, M. Chelnokov et al., Doubly magic nucleus $^{270}\text{Hs}_{162}$. *Phys. Rev. Lett.* **97**, 242501 (2006). <https://doi.org/10.1103/PhysRevLett.97.242501>
39. J. Dvorak, W. Brüchle, M. Chelnokov et al., Observation of the $3n$ evaporation channel in the complete Hot-Fusion reaction $^{26}\text{Mg} + ^{248}\text{Cm}$ leading to the new superheavy nuclide ^{271}Hs . *Phys. Rev. Lett.* **100**, 132503 (2008). <https://doi.org/10.1103/PhysRevLett.100.132503>
40. Y.T. Oganessian, V.K. Utyonkov, M.V. Shumeiko et al., Synthesis and decay properties of isotopes of element 110: ^{273}Ds and ^{275}Ds . *Phys. Rev. C* **109**, 054307 (2024). <https://doi.org/10.1103/PhysRevC.109.054307>
41. Y.A. Lazarev, Y.V. Lobanov, Y.T. Oganessian et al., α decay of $^{273}\text{110}$: shell closure at $N=162$. *Phys. Rev. C* **54**, 620–625 (1996). <https://doi.org/10.1103/PhysRevC.54.620>
42. V. Bernard, C. Gregoire, C. Mazur et al., Further experimental study of fast fission with the $\text{Cl} + \text{Au}$ system. *Nucl. Phys. A* **385**(2), 319–330 (1982). [https://doi.org/10.1016/0375-9474\(82\)90175-0](https://doi.org/10.1016/0375-9474(82)90175-0)
43. J.D. Bierman, P. Chan, J.F. Liang et al., Fusion barrier distributions for heavy ion systems involving prolate and oblate target nuclei. *Phys. Rev. C* **54**, 3068–3075 (1996). <https://doi.org/10.1103/PhysRevC.54.3068>
44. J.D. Bierman, P. Chan, J.F. Liang et al., Experimental fusion barrier distributions reflecting projectile octupole state coupling to prolate and oblate target nuclei. *Phys. Rev. Lett.* **76**, 1587–1590 (1996). <https://doi.org/10.1103/PhysRevLett.76.1587>
45. R. Vandenbosch, A.A. Sonzogni, J.D. Bierman, Effects of shape and transfer degrees of freedom on sub-barrier fusion. *J. Phys. G Nucl. Part. Phys.* **23**(10), 1303 (1997). <https://doi.org/10.1088/0954-3899/23/10/019>
46. M. Itkis, I. Itkis, G. Knyazheva et al., Fusion-fission and quasifission of superheavy systems in heavy-ion induced reactions. *Nucl. Phys. A* **834**(1), 374c–377c (2010). <https://doi.org/10.1016/j.nuclphysa.2010.01.043>
47. Y.T. Oganessian, Y.P. Tret'yakov, A.S. Il'inov et al., Synthesis of neutron-deficient isotopes of fermium, kurchatovium and element with atomic number 106. *JETP Lett.* **20**(8), 20 (1974)
48. Y.T. Oganessian, A.G. Demin, A.S. Il'inov et al., Experiments on the synthesis of neutron-deficient isotopes of kurchatovium in reactions with accelerated ^{50}Ti ions. *Sov. At. Energy* **38**(6), 492–501 (1975). <https://doi.org/10.1007/BF01127435>
49. A.G. Demin, S.P. Tretyakova, V.K. Utyonkov et al., On the properties of the element 106 isotopes produced in the reactions $\text{Pb} + ^{54}\text{Cr}$. *Zeitschrift für Physik A Atoms and Nucl.* **315**, 197–200 (1984). <https://doi.org/10.1007/BF01419379>
50. G. Münzenberg, S. Hofmann, F.P. Heßberger et al., Identification of element 107 by α correlation chains. *Z. Phys. A* **300**(1), 107–108 (1981). <https://doi.org/10.1007/BF01412623>
51. G. Münzenberg, P. Armbruster, H. Folger et al., The identification of element 108. *Z. Phys. A* **317**(2), 235–236 (1984). <https://doi.org/10.1007/BF01421260>
52. G. Münzenberg, P. Armbruster, F.P. Heßberger et al., Observation of one correlated- α -decay in the reaction ^{58}Fe on $^{209}\text{Bi} \rightarrow ^{267}\text{109}$. *Z. Phys. A: Hadrons Nucl.* **309**(1), 89–90 (1982). <https://doi.org/10.1007/BF01420157>
53. S. Hofmann, V. Ninov, F.P. Heßberger et al., Production and decay of $^{269}\text{110}$. *Z. Phys. A: Hadrons Nucl.* **350**(4), 277–280 (1995). <https://doi.org/10.1007/BF01291181>
54. S. Hofmann, V. Ninov, F.P. Heßberger et al., The new element 111. *Z. Phys. A: Hadrons Nucl.* **350**(4), 281–282 (1995). <https://doi.org/10.1007/BF01291182>

55. S. Hofmann, V. Ninov, F.P. Heßberger et al., The new element 112. *Z. Phys. A: Hadrons Nucl.* **354**(3), 229–230 (1996). <https://doi.org/10.1007/BF02769517>
56. F.P. Heßberger, S. Hofmann, V. Ninov et al., Spontaneous fission and alpha-decay properties of neutron deficient isotopes $^{257-253}$ 104 and 258 106. *Z. Phys. A: Hadrons Nucl.* **359**, 415–425 (1997). <https://doi.org/10.1007/s002180050422>
57. F.P. Heßberger, S. Hofmann, D. Ackermann et al., Decay properties of neutron-deficient isotopes 256,257 Db, 255 Rf, 252,253 Lr. *Eur. Phys. J. A* **12**, 57–67 (2001). <https://doi.org/10.1007/s10050017039>
58. F.P. Heßberger, G. Münzenberg, S. Hofmann et al., The new isotopes 258 105, 257 105, 254 Ir and 253 Lr. *Z. Phys. A* **322**, 557–566 (1985). <https://doi.org/10.1007/BF01415134>
59. G. Münzenberg, S. Hofmann, H. Folger et al., The isotopes 259 106, 260 106, and 261 106. *Z. Phys. A* **322**, 227–235 (1985). <https://doi.org/10.1007/BF01411887>
60. S. Hofmann, F.P. Heßberger, D. Ackermann et al., The new isotope 270 110 and its decay products 266 Hs and 262 Sg. *Eur. Phys. J. A* **10**, 5–10 (2001). <https://doi.org/10.1007/s100500170137>
61. G. Münzenberg, P. Armbruster, S. Hofmann et al., Element 107. *Z. Phys. A* **333**, 163–175 (1989). <https://doi.org/10.1007/BF01565147>
62. A. Ghiorso, D. Lee, L.P. Somerville et al., Evidence for the possible synthesis of element 110 produced by the $^{59}\text{Co} + ^{209}\text{Bi}$ reaction. *Phys. Rev. C* **51**, R2293–R2297 (1995). <https://doi.org/10.1103/PhysRevC.51.R2293>
63. Z.Y. Zhang, Z.G. Gan, L. Ma et al., Observation of the superheavy nuclide ^{271}Ds . *Chin. Phys. Lett.* **29**(1), 012502 (2012). <https://doi.org/10.1088/0256-307X/29/1/012502>
64. L.C. Sun, Z.Y. Zhang, Z.G. Gan et al., Systematics of production cross sections in ^{54}Cr -induced fusion evaporation reactions. *Phys. Rev. C* **110**(1), 014319 (2024). <https://doi.org/10.1103/PhysRevC.110.014319>
65. Y.T. Oganessian, A. Sobiczewski, G.M. Ter-Akopian, Superheavy nuclei: from predictions to discovery. *Phys. Script.* **92**(2), 023003 (2017). <https://doi.org/10.1088/1402-4896/aa53c1>
66. Y.A. Lazarev, Y.V. Lobanov, Y.T. Oganessian et al., Discovery of enhanced nuclear stability near the deformed shells $N = 162$ and $Z = 108$. *Phys. Rev. Lett.* **73**, 624–627 (1994). <https://doi.org/10.1103/PhysRevLett.73.624>
67. S. Hofmann, Synthesis of superheavy elements by cold fusion. *Radiochem. Acta* **99**(7–8), 405–428 (2011). <https://doi.org/10.1524/ract.2011.1854>
68. Y.T. Oganessian, V.K. Utyonkov, Y.V. Lobanov et al., Measurements of cross sections for the fusion-evaporation reactions $^{244}\text{Pu}(^{48}\text{Ca}, xn)^{292-x}114$ and $^{245}\text{Cm}(^{48}\text{Ca}, xn)^{293-x}116$. *Phys. Rev. C* **69**, 054607 (2004). <https://doi.org/10.1103/PhysRevC.69.054607>
69. J.H. Hamilton, S. Hofmann, Y.T. Oganessian, Search for superheavy nuclei. *Annu. Rev. Nucl. Part. Sci.* **63**(1), 383–405 (2013). <https://doi.org/10.1146/annurev-nucl-102912-144535>
70. R. Smolanczuk, J. Skalski, A. Sobiczewski, Spontaneous-fission half-lives of deformed superheavy nuclei. *Phys. Rev. C* **52**, 1871–1880 (1995). <https://doi.org/10.1103/PhysRevC.52.1871>
71. R. Smolanczuk, Properties of the hypothetical spherical superheavy nuclei. *Phys. Rev. C* **56**, 812–824 (1997). <https://doi.org/10.1103/PhysRevC.56.812>
72. Y.T. Oganessian, V.K. Utyonkov, Y.V. Lobanov et al., Synthesis of the isotope $^{282}\text{113}$ in the $^{237}\text{Np} + ^{48}\text{Ca}$ fusion reaction. *Phys. Rev. C* **76**, 011601 (2007). <https://doi.org/10.1103/PhysRevC.76.011601>
73. A. Såmark-Roth, D.M. Cox, D. Rudolph et al., Spectroscopy along flerovium decay chains: discovery of ^{280}Ds and an excited state in ^{282}Cn . *Phys. Rev. Lett.* **126**, 032503 (2021). <https://doi.org/10.1103/PhysRevLett.126.032503>
74. Y.T. Oganessian, V.K. Utyonkov, N.D. Kovrzhnykh et al., New isotope ^{286}Mc produced in the $^{243}\text{Am} + ^{48}\text{Ca}$ reaction. *Phys. Rev. C* **106**, 064306 (2022). <https://doi.org/10.1103/PhysRevC.106.064306>
75. Y.T. Oganessian, V.K. Utyonkov, M.V. Shumeiko et al., New isotope ^{276}Ds and its decay products ^{272}Hs and ^{268}Sg from the $^{232}\text{Th} + ^{48}\text{Ca}$ reaction. *Phys. Rev. C* **108**, 024611 (2023). <https://doi.org/10.1103/PhysRevC.108.024611>
76. <https://people.nscl.msu.edu/~thoennes/isotopes/index.html>
77. Y.T. Oganessian, V.K. Utyonkov, Super-heavy element research. *Rep. Prog. Phys.* **78**(3), 036301 (2015). <https://doi.org/10.1088/0034-4885/78/3/036301>
78. M. Thoennessen, Discovery of isotopes of elements with $Z \geq 100$. *At. Data Nucl. Data Tables* **99**(3), 312–344 (2013). <https://doi.org/10.1016/j.adt.2012.03.003>
79. G. Münzenberg, Super heavy elements—experimental developments. *EPJ Web Conf.* **182**, 02091 (2018). <https://doi.org/10.1051/epjconf/201818202091>
80. H.S. Xu, T.H. Huang, Z.Y. Sun et al., Status and prospect of super heavy nuclei research at IMP. *Nucl. Phys. Rev.* **23**(4), 359–368 (2006). <https://doi.org/10.11804/NuclPhysRev.23.04.359>
81. L.J. Mao, J.C. Yang, W.Q. Yang et al., Introduction of the heavy ion research facility in Lanzhou (HIRFL). *J. Instrum.* **15**(12), T12015 (2020). <https://doi.org/10.1088/1748-0221/15/12/T12015>
82. Y.J. Yuan, D.Q. Gao, L.Z. Ma et al., Present status of HIRFL complex in Lanzhou. *JINST* **1401**(1), 012003 (2020). <https://doi.org/10.1088/1742-6596/1401/1/012003>
83. M.H. Huang, Z.G. Gan, Z.Y. Zhang et al., α decay of the new isotope ^{204}Ac . *Phys. Lett. B* **834**, 137484 (2022). <https://doi.org/10.1016/j.physletb.2022.137484>
84. Z.Y. Zhang, Z.G. Gan, L. Ma et al., α decay of the new neutron-deficient isotope ^{205}Ac . *Phys. Rev. C* **89**, 014308 (2014). <https://doi.org/10.1103/PhysRevC.89.014308>
85. H.B. Yang, Z.G. Gan, Z.Y. Zhang et al., New isotope ^{207}Th and odd-even staggering in α -decay energies for nuclei with $Z > 82$ and $N < 126$. *Phys. Rev. C* **105**, L051302 (2022). <https://doi.org/10.1103/PhysRevC.105.L051302>
86. Z.Y. Zhang, H.B. Yang, M.H. Huang et al., New α -emitting isotope ^{214}U and abnormal enhancement of α -particle clustering in lightest uranium isotopes. *Phys. Rev. Lett.* **126**, 152502 (2021). <https://doi.org/10.1103/PhysRevLett.126.152502>
87. L. Ma, Z.Y. Zhang, Z.G. Gan et al., α -decay properties of the new isotope ^{216}U . *Phys. Rev. C* **91**, 051302 (2015). <https://doi.org/10.1103/PhysRevC.91.051302>
88. H.B. Yang, L. Ma, Z.Y. Zhang et al., Alpha decay properties of the semi-magic nucleus ^{219}Np . *Phys. Lett. B* **777**, 212–216 (2018). <https://doi.org/10.1016/j.physletb.2017.12.017>
89. Z.Y. Zhang, Z.G. Gan, H.B. Yang et al., New isotope ^{220}Np : probing the robustness of the $N = 126$ shell closure in neptunium. *Phys. Rev. Lett.* **122**, 192503 (2019). <https://doi.org/10.1103/PhysRevLett.122.192503>
90. L. Ma, Z.Y. Zhang, Z.G. Gan et al., Short-lived α -emitting isotope ^{222}Np and the stability of the $N = 126$ magic shell. *Phys. Rev. Lett.* **125**, 032502 (2020). <https://doi.org/10.1103/PhysRevLett.125.032502>
91. M.D. Sun, Z. Liu, T. Huang et al., New short-lived isotope ^{223}Np and the absence of the $Z=92$ subshell closure near $N = 126$. *Phys. Lett. B* **771**, 303–308 (2017). <https://doi.org/10.1016/j.physletb.2017.03.074>

92. T.H. Huang, W.Q. Zhang, M.D. Sun et al., Identification of the new isotope ^{224}Np . Phys. Rev. C **98**, 044302 (2018). <https://doi.org/10.1103/PhysRevC.98.044302>
93. Z.G. Gan, W.X. Huang, Z.Y. Zhang et al., Results and perspectives for study of heavy and super-heavy nuclei and elements at IMP/CAS. Eur. Phys. J. A **58**(8), 158 (2022). <https://doi.org/10.1140/epja/s10050-022-00811-w>
94. H.B. Yang, Z.G. Gan, Y.J. Li et al., Discovery of new isotopes ^{160}Os and ^{156}W : revealing enhanced stability of the $N = 82$ shell closure on the neutron-deficient side. Phys. Rev. Lett. **132**, 072502 (2024). <https://doi.org/10.1103/PhysRevLett.132.072502>
95. J.G. Wang, Z.G. Gan, Z.Y. Zhang et al., α -decay properties of new neutron-deficient isotope ^{203}Ac . Phys. Lett. B **850**, 138503 (2024). <https://doi.org/10.1016/j.physletb.2024.138503>
96. R. Singh, Longitudinal beam diagnostics R & D at GSI-UNILAC, in *15th International Conference on Heavy Ion Accelerator Technology* (HIAT'22), pp. 144–149 (2022). <https://doi.org/10.18429/JACoW-HIAT2022-TH2I2>
97. W. Barth, A. Adonin, C.E. Düllmann et al., High brilliance uranium beams for the GSI FAIR. Phys. Rev. Accel. Beams **20**, 050101 (2017). <https://doi.org/10.1103/PhysRevAccelBeams.20.050101>
98. W. Barth, U. Scheeler, H. Vormann et al., High brilliance beam investigations at the universal linear accelerator. Phys. Rev. Accel. Beams **25**, 040101 (2022). <https://doi.org/10.1103/PhysRevAccelBeams.25.040101>
99. W. Barth, W. Bayer, L. Dahl et al., Upgrade program of the high current heavy ion UNILAC as an injector for FAIR. Nucl. Instrum. Methods Phys. Res. A **577**(1), 211–214 (2007). <https://doi.org/10.1016/j.nima.2007.02.054>
100. F.S. Zhang, Y.H. Zhang, M.H. Zhang et al., Synthesis of new superheavy nuclei. J. Beijing Norm. Univ. (Nat. Sci.) **58**(3), 392–399 (2022). <https://doi.org/10.1220/j.0476-0301.20220282>
101. H. Sakai, P. Brionnet, SHE Research at RIKEN Nishina Center. Acta. Phys. Polon. Supp. **17**(3), 3-A21 (2024). <https://doi.org/10.5506/APhysPolBSupp.17.3-A21>
102. H. Sakai, H. Haba, K. Morimoto et al., Facility upgrade for superheavy-element research at RIKEN. Eur. Phys. J. A **58**(12), 238 (2022). <https://doi.org/10.1140/epja/s10050-022-00888-3>
103. G.G. Gulbekian, S.N. Dmitriev, M.G. Itkis et al., Start-Up of the DC-280 cyclotron, the basic facility of the factory of super-heavy elements of the laboratory of nuclear reactions at the joint institute for nuclear research. Phys. Part. Nucl. Lett. **16**, 866–875 (2019). <https://doi.org/10.1134/S1547477119060177>
104. V. Semin, S. Bogomolov, K. Gikal et al., DC-280 cyclotron for factory of super heavy elements experimental results, in *Proceedings of 12th International Particle Accelerator Conference (IPAC2021)* (2021), pp. 4126–4129. <https://doi.org/10.18429/JACoW-IPAC2021-THPAB182>
105. G. Gulbekian, S. Dmitriev, Y.T. Oganessian et al., The new DC-280 cyclotron. Status and road map. Phys. Part. Nucl. Lett. **15**, 809–813 (2018). <https://doi.org/10.1134/S1547477118070773>
106. M. Khabarov, SHE factory: cyclotron facility for Super Heavy Elements Research, in *International Conference on Cyclotrons and their Applications* (22nd) (2020)
107. M.K. Covo, R.A. Albright, B.F. Ninemire et al., The 88-Inch Cyclotron: a one-stop facility for electronics radiation and detector testing. Measure **127**, 580–587 (2018). <https://doi.org/10.1016/j.measurement.2017.10.018>
108. P. Ostroumov, M. Hausmann, K. Fukushima et al., Heavy ion beam physics at Facility for Rare Isotope Beams. J. Instrum. **15**(12), P12034 (2020). <https://doi.org/10.1088/1748-0221/15/12/P12034>
109. H.L. Crawford, V. Tripathi, J.M. Allmond et al., Crossing $N = 28$ toward the neutron drip line: first measurement of Half-Lives at FRIB. Phys. Rev. Lett. **129**, 212501 (2022). <https://doi.org/10.1103/PhysRevLett.129.212501>
110. P.N. Ostroumov, O.B. Tarasov, N. Bultman et al., Acceleration of uranium beam to record power of 10.4 kW and observation of new isotopes at Facility for Rare Isotope Beams. Phys. Rev. Accel. Beams **27**, 060101 (2024). <https://doi.org/10.1103/PhysRevAccelBeams.27.060101>
111. J. Wei, H. Ao, B. Arend et al., Accelerator commissioning and rare isotope identification at the facility for rare isotope beams. Mod. Phys. Lett. **37**(09), 2230006 (2022). <https://doi.org/10.1142/S0217732322300063>
112. X.H. Zhou, J.C. Yang, H.P. Team, Status of the high-intensity heavy-ion accelerator facility in China. AAPPS Bull. **32**(1), 35 (2022). <https://doi.org/10.1007/s43673-022-00064-1>
113. J.J. Zhang, Z.Y. Xu, J.Q. Zhang et al., Design study of charge-stripping scheme of heavy ion beams for HIAF-BRing. Nucl. Sci. Tech. **35**(5), 46 (2024). <https://doi.org/10.1007/s41365-024-01397-2>
114. Z.Y. Sun, J.C. Yang, Y.T. Zhao et al., Huizhou accelerator complex facility and its future development. Sci. Sin.-Phys. Mech. Astron. **50**(11), 112006 (2020). <https://doi.org/10.1360/SSPMA-2020-0248>
115. X. Ma, W. Wen, S. Zhang et al., HIAF New opportunities for atomic physics with highly charged heavy ions. Nucl. Instrum. Methods Phys. Res. Sect. B **408**, 169–173 (2017). <https://doi.org/10.1016/j.nimb.2017.03.129>
116. P. Spiller, R. Balss, P. Bartolome et al., The FAIR heavy ion synchrotron SIS100. J. Instrum. **15**(12), T12013 (2020). <https://doi.org/10.1088/1748-0221/15/12/T12013>
117. A.V. Butenko, O.I. Brovko, A.R. Galimov et al., NICA Booster: a new-generation superconducting synchrotron. Usp. Fiz. Nauk **193**(2), 206–225 (2023). <https://doi.org/10.3367/UFNe.2021.12.039138>
118. Y. Blumenfeld, P. Butler, J. Cornell et al., Eurisol design study: towards an Ultimate ISOL Facility for Europe. Int. J. Mod. Phys. E **18**(10), 1960–1964 (2009). <https://doi.org/10.1142/S0218301309014081>
119. Y.T. Oganessian, Nuclei in the “Island of Stability” of super-heavy elements. J. Phys. Conf. Ser. **337**, 012005 (2012). <https://doi.org/10.1088/1742-6596/337/1/012005>
120. S. Heinz, Research at SHIP—status and perspectives. EPJ Web Conf. **38**, 01002 (2012). <https://doi.org/10.1051/epjconf/20123801002>
121. A.G. Popeko, A.V. Yeremin, O.N. Malyshev et al., Separator for heavy element spectroscopy–velocity filter SHELs. Nucl. Instrum. Methods Phys. Res. Sect. B **376**, 140–143 (2016). <https://doi.org/10.1016/j.nimb.2016.03.045>
122. Y.T. Oganessian, V.K. Utyonkov, A.G. Popeko et al., DGFRS-2—a gas-filled recoil separator for the Dubna super heavy element factory. Nucl. Instrum. Methods Phys. Res. Sect. A **1033**, 166640 (2022). <https://doi.org/10.1016/j.nima.2022.166640>
123. A. Semchenkov, W. Brüchle, E. Jäger et al., The TransActinide separator and chemistry apparatus (TASCA) at GSI—Optimization of ion-optical structures and magnet designs. Nucl. Instrum. Methods Phys. Res. Sect. B **266**(19), 4153–4161 (2008). <https://doi.org/10.1016/j.nimb.2008.05.132>
124. V. Ninov, K. Gregorich, C. McGrath, The Berkeley gas-filled separator, in *AIP Conference Proceedings*, Vol. 455, American Institute of Physics, (1998), pp. 704–707. <https://doi.org/10.1063/1.57362>
125. D. Kaji, K. Morimoto, N. Sato et al., Gas-filled recoil ion separator GARIS-II. Nucl. Instrum. Methods Phys. Res. Sect. B **317**, 311–314 (2013). <https://doi.org/10.1016/j.nimb.2013.05.085>

126. W.L. Zhan, J.W. Xia, H.W. Zhao et al., HIRFL Today. *Nucl. Phys. A* **805**(1), 533c–540c (2008). <https://doi.org/10.1016/j.nuclphysa.2008.02.292>
127. J.M. Gates, C.E. Düllmann, M. Schädel et al., First superheavy element experiments at the GSI recoil separator TASCA: the production and decay of element 114 in the $^{244}\text{Pu} + ^{48}\text{Ca}, 3-4n$ reaction. *Phys. Rev. C* **83**, 054618 (2011). <https://doi.org/10.1103/PhysRevC.83.054618>
128. P. Brionnet, R.K. Grzywacz, D. Kaji et al., Development of digital electronics for the search of SHE nuclei using GARIS-II/III at RIKEN. *Nucl. Instrum. Methods Phys. Res. Sect. A* **1049**, 168068 (2023). <https://doi.org/10.1016/j.nima.2023.168068>
129. L.N. Sheng, Q. Hu, H. Jia et al., Ion-optical design and multiparticle tracking in 3D magnetic field of the gas-filled recoil separator SHANS2 at CAFE2. *Nucl. Instrum. Methods Phys. Res. Sect. A* **1004**, 165348 (2021). <https://doi.org/10.1016/j.nima.2021.165348>
130. S.Y. Xu, Z.Y. Zhang, Z.G. Gan et al., A gas-filled recoil separator, SHANS2, at the China Accelerator Facility for Superheavy Elements. *Nucl. Instrum. Methods Phys. Res. Sect. A* **1050**, 168113 (2023). <https://doi.org/10.1016/j.nima.2023.168113>
131. Y.H. Zhang, G. Zhang, J.J. Li et al., Production cross sections of $^{243-248}\text{No}$ isotopes in fusion reactions. *Phys. Rev. C* **106**, 014625 (2022). <https://doi.org/10.1103/PhysRevC.106.014625>
132. N. Wang, Z.X. Li, X.Z. Wu, Improved quantum molecular dynamics model and its applications to fusion reaction near barrier. *Phys. Rev. C* **65**, 064608 (2002). <https://doi.org/10.1103/PhysRevC.65.064608>
133. L.L. Zhou, J.J. Cai, L.Q. Li et al., Fusion enhancement in the collisions with ^{44}Ca beams and the production of neutron-deficient $^{245-250}\text{Lr}$ isotopes. *Phys. Rev. C* **109**, 024606 (2024). <https://doi.org/10.1103/PhysRevC.109.024606>
134. X.X. Sun, L. Guo, Microscopic study of the hot-fusion reaction $^{48}\text{Ca} + ^{238}\text{U}$ with the constraints from time-dependent hartree-fock theory. *Phys. Rev. C* **107**, 064609 (2023). <https://doi.org/10.1103/PhysRevC.107.064609>
135. P. Magierski, K. Sekizawa, G. Włazłowski, Novel role of superfluidity in low-energy nuclear reactions. *Phys. Rev. Lett.* **119**, 042501 (2017). <https://doi.org/10.1103/PhysRevLett.119.042501>
136. A.S. Umar, V.E. Oberacker, J.A. Maruhn et al., Entrance channel dynamics of hot and cold fusion reactions leading to superheavy elements. *Phys. Rev. C* **81**, 064607 (2010). <https://doi.org/10.1103/PhysRevC.81.064607>
137. K. Sekizawa, K. Hagino, Time-dependent Hartree-Fock plus Langevin approach for hot fusion reactions to synthesize the $Z = 120$ superheavy element. *Phys. Rev. C* **99**, 051602(R) (2019). <https://doi.org/10.1103/PhysRevC.99.051602>
138. H. Yao, H. Yang, N. Wang, Systematic study of capture thresholds with time dependent Hartree-Fock theory. *Phys. Rev. C* **110**, 014602 (2024). <https://doi.org/10.1103/PhysRevC.110.014602>
139. Z.H. Liu, J.D. Bao, Synthesis of superheavy element 120 via $^{50}\text{Ti} + ^4\text{Cf}$ hot fusion reactions. *Phys. Rev. C* **80**, 054608 (2009). <https://doi.org/10.1103/PhysRevC.80.054608>
140. K. Siwek-Wilczyńska, T. Cap, M. Kowal, Exploring the production of new superheavy nuclei with proton and α -particle evaporation channels. *Phys. Rev. C* **99**, 054603 (2019). <https://doi.org/10.1103/PhysRevC.99.054603>
141. S. Chopra, M.K. Sharma, P.O. Hess et al., Possibility to form $Z = 120$ via the $^{64}\text{Ni} + ^{238}\text{U}$ reaction using the dynamical cluster-decay model. *Phys. Rev. C* **105**, 014610 (2022). <https://doi.org/10.1103/PhysRevC.105.014610>
142. S. Chopra, P.O. Hess, Predicted cross sections for the synthesis of $Z = 120$ fusion via $^{54}\text{Cr} + ^{248}\text{Cm}$ and $^{50}\text{Ti} + ^{249}\text{Cf}$ target-projectile combinations. *Phys. Rev. C* **110**, 014615 (2024). <https://doi.org/10.1103/PhysRevC.110.014615>
143. L. Liu, C.W. Shen, Q.F. Li et al., Residue cross sections of ^{50}Ti -induced fusion reactions based on the two-step model. *Eur. Phys. J. A* **52**, 35–39 (2016). <https://doi.org/10.1140/epja/i2016-16035-0>
144. C.W. Shen, Y. Abe, D. Boilley et al., Isospin dependence of reactions $^{48}\text{Ca} + ^{243-251}\text{Bk}$. *Int. J. Mod. Phys. E* **17**, 66–79 (2008). <https://doi.org/10.1142/S0218301308011768>
145. D. Boilley, Y. Abe, B. Cauchois et al., Elimination of fast variables and initial slip: a new mechanism for fusion hindrance in heavy-ion collisions. *J. Phys. G Nucl. Part. Phys.* **46**(11), 115102 (2019). <https://doi.org/10.1088/1361-6471/ab11ef>
146. H.L. Lü, D. Boilley, Y. Abe et al., Synthesis of superheavy elements: Uncertainty analysis to improve the predictive power of reaction models. *Phys. Rev. C* **94**, 034616 (2016). <https://doi.org/10.1103/PhysRevC.94.034616>
147. V.Y. Denisov, Model for compound nucleus formation in various heavy-ion systems. *Phys. Rev. C* **109**, 014607 (2024). <https://doi.org/10.1103/PhysRevC.109.014607>
148. V.I. Zagrebaev, W. Greiner, Cross sections for the production of superheavy nuclei. *Nucl. Phys. A* **944**, 257–307 (2015). <https://doi.org/10.1016/j.nuclphysa.2015.02.010>
149. V.L. Litnevsky, G.I. Kosenko, F.A. Ivanyuk, Description of fusion and evaporation residue formation cross sections in reactions leading to the formation of element $Z = 122$ within the Langevin approach. *Phys. Rev. C* **93**, 064606 (2016). <https://doi.org/10.1103/PhysRevC.93.064606>
150. S. Amano, Y. Aritomo, M. Ohta, Dynamical mechanism of fusion hindrance in heavy ion collisions. *Phys. Rev. C* **108**, 014612 (2023). <https://doi.org/10.1103/PhysRevC.108.014612>
151. S. Amano, Y. Aritomo, M. Ohta, Effects of neck and nuclear orientations on the mass drift in heavy ion collisions. *Phys. Rev. C* **109**, 034603 (2024). <https://doi.org/10.1103/PhysRevC.109.034603>
152. N. Wang, E.G. Zhao, W. Scheid et al., Theoretical study of the synthesis of superheavy nuclei with $Z = 119$ and 120 in heavy-ion reactions with trans-uranium targets. *Phys. Rev. C* **85**, 041601(R) (2012). <https://doi.org/10.1103/PhysRevC.85.041601>
153. X.J. Bao, Y. Gao, J.Q. Li et al., Influence of the nuclear dynamical deformation on production cross sections of superheavy nuclei. *Phys. Rev. C* **91**, 011603 (2015). <https://doi.org/10.1103/PhysRevC.91.011603>
154. Z.Q. Feng, G.M. Jin, F. Fu et al., Production cross sections of superheavy nuclei based on dinuclear system model. *Nucl. Phys. A* **771**, 50–67 (2006). <https://doi.org/10.1016/j.nuclphysa.2006.03.002>
155. L. Zhu, Z.Q. Feng, C. Li et al., Orientation effects on evaporation residue cross sections in ^{48}Ca -induced hot fusion reactions. *Phys. Rev. C* **90**, 014612 (2014). <https://doi.org/10.1103/PhysRevResearch.5.L022030>
156. M.H. Zhang, Y.H. Zhang, Y. Zou et al., Possibilities for the synthesis of superheavy element $Z = 121$ in fusion reactions. *Nucl. Sci. Tech.* **35**(6), 95 (2024). <https://doi.org/10.1007/s41365-024-01452-y>
157. M.H. Zhang, Y.H. Zhang, Y. Zou et al., Predictions of synthesizing elements with $Z = 119$ and 120 in fusion reactions. *Phys. Rev. C* **109**, 014622 (2024). <https://doi.org/10.1103/PhysRevC.109.014622>
158. L.Q. Li, G. Zhang, F.S. Zhang, Production of unknown Fl isotopes in proton evaporation channels within the dinuclear system model. *Phys. Rev. C* **106**, 024601 (2022). <https://doi.org/10.1103/PhysRevC.106.024601>

159. Z.H. Wu, L. Zhu, F. Li et al., Synthesis of neutron-rich superheavy nuclei with radioactive beams within the dinuclear system model. *Phys. Rev. C* **97**, 064609 (2018). <https://doi.org/10.1103/PhysRevC.97.064609>
160. Q.F. Li, W. Zuo, W.F. Li et al., Deformation and orientation effects in the driving potential of the dinuclear model. *Eur. Phys. J. A* **24**(2), 223–229 (2005). <https://doi.org/10.1140/epja/i2004-10138-1>
161. S.Y. Xu, Z.Q. Feng, Cluster emission in massive transfer reactions based on dinuclear system model. *Nucl. Tech. (in Chinese)* **46**, 030501 (2023). <https://doi.org/10.11889/j.0253-3219.2023.hjs.46.030501>
162. C. Simenel, A.S. Umar, Heavy-ion collisions and fission dynamics with the time-dependent Hartree–Fock theory and its extensions. *Prog. Part. Nucl. Phys.* **103**, 19–66 (2018). <https://doi.org/10.1016/j.ppnp.2018.07.002>
163. K. Sekizawa, TDHF theory and its extensions for the multi-nucleon transfer reaction: a mini review. *Front. Phys.* **7**, 20 (2019). <https://doi.org/10.3389/fphy.2019.00020>
164. A.S. Umar, V.E. Oberacker, C. Simenel, Fusion and quasifission dynamics in the reactions $^{48}\text{Ca} + ^{249}\text{Bk}$ and $^{50}\text{Ti} + ^{249}\text{Bk}$ using a time-dependent Hartree–Fock approach. *Phys. Rev. C* **94**, 024605 (2016). <https://doi.org/10.1103/PhysRevC.94.024605>
165. L. Guo, C.W. Shen, C. Yu et al., Isotopic trends of quasifission and fusion-fission in the reactions $^{48}\text{Ca} + ^{239,244}\text{Pu}$. *Phys. Rev. C* **98**, 064609 (2018). <https://doi.org/10.1103/PhysRevC.98.064609>
166. H. Wolter, M. Colonna, D. Cozma et al., Transport model comparison studies of intermediate-energy heavy-ion collisions. *Prog. Part. Nucl. Phys.* **125**, 103962 (2022). <https://doi.org/10.1016/j.ppnp.2022.103962>
167. J. Aichelin, “quantum” molecular dynamics—a dynamical microscopic n-body approach to investigate fragment formation and the nuclear equation of state in heavy ion collisions. *Phys. Rep.* **202**(5), 233–360 (1991). [https://doi.org/10.1016/0370-1573\(91\)90094-3](https://doi.org/10.1016/0370-1573(91)90094-3)
168. A.S. Zubov, G.G. Adamian, N.V. Antonenko et al., Survival probability of superheavy nuclei. *Phys. Rev. C* **65**, 024308 (2002). <https://doi.org/10.1103/PhysRevC.65.024308>
169. T.L. Zhao, X.J. Bao, H.F. Zhang, Exploring the optimal way to produce $Z = 100–106$ neutron-rich nuclei. *Phys. Rev. C* **108**, 024602 (2023). <https://doi.org/10.1103/PhysRevC.108.024602>
170. N. Wang, K. Zhao, W. Scheid et al., Fusion-fission reactions with a modified Woods–Saxon potential. *Phys. Rev. C* **77**, 014603 (2008). <https://doi.org/10.1103/PhysRevC.77.014603>
171. H.L. Lü, A. Marchix, Y. Abe et al., KEWPIE2: a cascade code for the study of dynamical decay of excited nuclei. *Comput. Phys. Commun.* **200**, 381–399 (2016). <https://doi.org/10.1016/j.cpc.2015.12.003>
172. W.J. Swiatecki, Three lectures on macroscopic aspects of nuclear dynamics. *Prog. Part. Nucl. Phys.* **4**, 383–450 (1980). [https://doi.org/10.1016/0146-6410\(80\)90014-9](https://doi.org/10.1016/0146-6410(80)90014-9)
173. S. Bjornholm, W.J. Swiatecki, Dynamical aspects of nucleus–nucleus collisions. *Nucl. Phys. A* **391**, 471–504 (1982). [https://doi.org/10.1016/0375-9474\(82\)90621-2](https://doi.org/10.1016/0375-9474(82)90621-2)
174. W.J. Swiatecki, The dynamics of the fusion of two nuclei. *Nucl. Phys. A* **376**(2), 275–291 (1982). [https://doi.org/10.1016/0375-9474\(82\)90065-3](https://doi.org/10.1016/0375-9474(82)90065-3)
175. J.P. Blocki, H. Feldmeier, W.J. Swiatecki, Dynamical hindrance to compound-nucleus formation in heavy-ion reactions. *Nucl. Phys. A* **459**(1), 145–172 (1986). [https://doi.org/10.1016/0375-9474\(86\)90061-8](https://doi.org/10.1016/0375-9474(86)90061-8)
176. V.V. Volkov, What is the most realistic mechanism of the compound nucleus formation in the complete fusion of two massive nuclei? *Acta Phys. Hungar. Ser. A: Heavy Ion Phys.* **19**, 67–75 (2004). <https://doi.org/10.1556/APH.19.2004.1-2.10>
177. C.W. Shen, Y. Abe, D. Boilley et al., Isospin dependence of reactions $^{48}\text{Ca} + ^{243–251}\text{Bk}$. *Int. J. Mod. Phys. E* **17**, 66–79 (2008). <https://doi.org/10.1142/S0218301308011768>
178. K. Hagino, Hot fusion reactions with deformed nuclei for synthesis of superheavy nuclei: an extension of the fusion-by-diffusion model. *Phys. Rev. C* **98**, 014607 (2018). <https://doi.org/10.1103/PhysRevC.98.014607>
179. M.H. Zhang, Y.H. Zhang, J.J. Li et al., Progress in transport models of heavy-ion collisions for the synthesis of superheavy nuclei. *Nucl. Tech. (in Chinese)* **46**(08), 080014 (2023). <https://doi.org/10.11889/j.0253-3219.2023.hjs.46.080014>
180. M.H. Zhang, M.C. Wang, Z. Zou et al., Predictions for the synthesis of unknown $^{279–281}\text{Nh}$ and $^{287,288}\text{Nh}$ isotopes. *Phys. Rev. C* **111**, 024611 (2025). <https://doi.org/10.1103/PhysRevC.111.024611>
181. J.X. Li, H.F. Zhang, Evaporation residue cross sections of superheavy nuclei based on optimized nuclear data. *Chin. Phys. C* **47**(12), 124105 (2023). <https://doi.org/10.1088/1674-1137/ad021f>
182. Y.P. Fang, Z.P. Gao, Y.N. Zhang et al., Bayesian uncertainty quantification for synthesizing superheavy elements. *Phys. Lett. B* **858**, 139069 (2024). <https://doi.org/10.1016/j.physletb.2024.139069>
183. Z.P. Gao, S.Y. Liu, P.W. Wen et al., Constraining the Woods–Saxon potential in fusion reactions based on the neural network. *Phys. Rev. C* **109**, 024601 (2024). <https://doi.org/10.1103/PhysRevC.109.024601>
184. W.H. Ye, Y.B. Qian, H.K. Wang, Multiple constraints on nuclear mass formulas for reliable extrapolations. *Phys. Rev. C* **107**(4), 044302 (2023). <https://doi.org/10.1103/PhysRevC.107.044302>
185. V.I. Zagrebaev, Synthesis of superheavy nuclei: nucleon collectivization as a mechanism for compound nucleus formation. *Phys. Rev. C* **64**, 034606 (2001). <https://doi.org/10.1103/PhysRevC.64.034606>
186. X.J. Lv, Z.Y. Yue, W.J. Zhao et al., Theoretical study of evaporation-residue cross sections of superheavy nuclei. *Phys. Rev. C* **103**, 064616 (2021). <https://doi.org/10.1103/PhysRevC.103.064616>
187. V. Zagrebaev, W. Greiner, Synthesis of superheavy nuclei: a search for new production reactions. *Phys. Rev. C* **78**, 034610 (2008). <https://doi.org/10.1103/PhysRevC.78.034610>
188. N. Wang, J.L. Tian, W. Scheid, Systematics of fusion probability in “hot” fusion reactions. *Phys. Rev. C* **84**, 061601 (2011). <https://doi.org/10.1103/PhysRevC.84.061601>
189. L. Zhu, W.J. Xie, F.S. Zhang, Production cross sections of superheavy elements $Z = 119$ and 120 in hot fusion reactions. *Phys. Rev. C* **89**, 024615 (2014). <https://doi.org/10.1103/PhysRevC.89.024615>
190. W. Loveland, Synthesis of transactinide nuclei using radioactive beams. *Phys. Rev. C* **76**, 014612 (2007). <https://doi.org/10.1103/PhysRevC.76.014612>
191. N.V. Antonenko, E.A. Cherepanov, A.K. Nasirov et al., Compound nucleus formation in reactions between massive nuclei: fusion barrier. *Phys. Rev. C* **51**, 2635–2645 (1995). <https://doi.org/10.1103/PhysRevC.51.2635>
192. L. Zhu, Law of optimal incident energy for synthesizing superheavy elements in hot fusion reactions. *Phys. Rev. Res.* **5**, L022030 (2023). <https://doi.org/10.1103/PhysRevResearch.5.L022030>
193. https://www.gsi.de/en/work/forschung/nustarena/nustarena_divisions/she_physik/research/super_heavy_elements/element_120

194. Y.T. Oganessian, V.K. Utyonkov, Y.V. Lobanov et al., Attempt to produce element 120 in the $^{244}\text{Pu} + ^{58}\text{Fe}$ reaction. *Phys. Rev. C* **79**, 024603 (2009). <https://doi.org/10.1103/PhysRevC.79.024603>
195. S. Hofmann, S. Heinz, R. Mann et al., Remarks on the fission barriers of super-heavy nuclei. *Eur. Phys. J. A* **52**(6), 116 (2016). <https://doi.org/10.1140/epja/i2016-16116-0>
196. S. Hofmann, S. Heinz, R. Mann et al., Review of even element super-heavy nuclei and search for element 120. *Eur. Phys. J. A* **52**, 180 (2016). <https://doi.org/10.1140/epja/i2016-16180-4>
197. F.P. Heßberger, D. Ackermann, Some critical remarks on a sequence of events interpreted to possibly originate from a decay chain of an element 120 isotope. *Eur. Phys. J. A* **53**(6), 123 (2017). <https://doi.org/10.1140/epja/i2017-12307-5>
198. J. Khuyagbaatar, A. Yakushev, C.E. Düllmann et al., Search for elements 119 and 120. *Phys. Rev. C* **102**, 064602 (2020). <https://doi.org/10.1103/PhysRevC.102.064602>
199. M. Tanaka, P. Brionnet, M. Du et al., Probing optimal reaction energy for synthesis of element 119 from $^{51}\text{V} + ^{248}\text{Cm}$ reaction with quasielastic barrier distribution measurement. *J. Phys. Soc. Jpn.* **91**(8), 084201 (2022). <https://doi.org/10.7566/JPSJ.91.084201>
200. J.M. Gates, R. Orford, D. Rudolph et al., Toward the discovery of new elements: production of livermorium ($Z = 116$) with ^{50}Ti . *Phys. Rev. Lett.* **133**(17), 172502 (2024). <https://doi.org/10.1103/PhysRevLett.133.172502>
201. K. Bourzac, Heaviest element yet within reach after major breakthrough. *Nature* **632**(8023), 16–17 (2024). <https://doi.org/10.1038/d41586-024-02416-3>
202. J.B. Roberto, M. Du, J.G. Ezold et al., Actinide targets for the synthesis of superheavy nuclei. *Eur. Phys. J. A* **59**(12), 304 (2023). <https://doi.org/10.1140/epja/s10050-023-01144-y>
203. N. Ghahramany, A. Ansari, Synthesis and decay process of superheavy nuclei with $Z = 119–122$ via hot-fusion reactions. *Eur. Phys. J. A* **52**(9), 287 (2016). <https://doi.org/10.1140/epja/i2016-16287-6>
204. X.Q. Deng, S.G. Zhou, Examination of promising reactions with ^{241}Am and ^{244}Cm targets for the synthesis of new superheavy elements within the dinuclear system model with a dynamical potential energy surface. *Phys. Rev. C* **107**, 014616 (2023). <https://doi.org/10.1103/PhysRevC.107.014616>
205. K.V. Novikov, E.M. Kozulin, G.N. Knyazheva et al., Investigation of fusion probabilities in the reactions with $^{52,54}\text{Cr}$, ^{64}Ni , and ^{68}Zn ions leading to the formation of $Z = 120$ superheavy composite systems. *Phys. Rev. C* **102**, 044605 (2020). <https://doi.org/10.1103/PhysRevC.102.044605>
206. G.G. Adamian, N.V. Antonenko, Optimal ways to produce heavy and superheavy nuclei. *Eur. Phys. J. A* **58**(6), 111 (2022). <https://doi.org/10.1140/epja/s10050-022-00764-0>
207. Z.G. Gan, X.H. Zhou, M.H. Huang et al., Predictions of synthesizing element 119 and 120. *Sci. Chin. Phys. Mech.* **54**, 61–66 (2011). <https://doi.org/10.1007/s11433-011-4436-4>
208. S. Kaur, M.K. Sharma, R. Kumar, Systematic study of probable target-projectile combinations for the synthesis of $Z = 120$ isotopes using the Skyrme energy density formalism. *Nucl. Phys. A* **1027**, 122491 (2022). <https://doi.org/10.1016/j.nuclphysa.2022.122491>
209. V.I. Zagrebaev, A.V. Karpov, W. Greiner, Possibilities for synthesis of new isotopes of superheavy elements in fusion reactions. *Phys. Rev. C* **85**, 014608 (2012). <https://doi.org/10.1103/PhysRevC.85.014608>
210. A. Nasirov, B. Kayumov, Optimal colliding energy for the synthesis of a superheavy element with $Z = 119$. *Phys. Rev. C* **109**, 024613 (2024). <https://doi.org/10.1103/PhysRevC.109.024613>
211. H.M. Albers, J. Khuyagbaatar, D.J. Hinde et al., Zeptosecond contact times for element $Z=120$ synthesis. *Phys. Lett. B* **808**, 135626 (2020). <https://doi.org/10.1016/j.physletb.2020.135626>
212. C. Borcea, Y.E. Penionzhkevich, S. Lukyanov, High energy alpha particle emission as a challenging mechanism for synthesis of very heavy nuclei. *J. Phys. Conf. Ser.* **1643**(1), 012072 (2020). <https://doi.org/10.1088/1742-6596/1643/1/012072>
213. B.S. Cai, C.X. Yuan, Random forest-based prediction of decay modes and half-lives of superheavy nuclei. *Nucl. Sci. Tech.* **34**, 204 (2023). <https://doi.org/10.1007/s41365-023-01354-5>
214. Z. Wang, Z.Z. Ren, Predictions of the decay properties of the superheavy nuclei $^{293,294}119$ and $^{294,295}120$. *Nucl. Technol.* **46**, 114 (2023). <https://doi.org/10.11889/j.0253-3219.2023.hjs.46.080011>
215. D.W. Guan, J.C. Pei, High quality microscopic nuclear masses of superheavy nuclei. *Phys. Lett. B* **851**, 138578 (2024). <https://doi.org/10.1016/j.physletb.2024.138578>
216. W.H. Ye, Y.B. Qian, Z.Z. Ren, Accuracy versus predictive power in nuclear mass tabulations. *Phys. Rev. C* **106**(2), 024318 (2022). <https://doi.org/10.1103/PhysRevC.106.024318>
217. W.H. Ye, Y.B. Qian, Z.Z. Ren, Refining the nuclear mass model via the α decay energy. *Phys. Rev. C* **104**(6), 064308 (2021). <https://doi.org/10.1103/PhysRevC.104.064308>
218. X.J. Bao, Y. Gao, J.Q. Li et al., Influence of nuclear basic data on the calculation of production cross sections of superheavy nuclei. *Phys. Rev. C* **92**, 014601 (2015). <https://doi.org/10.1103/PhysRevC.92.014601>
219. C. Geng, P.H. Chen, F. Niu et al., Assessing the impact of nuclear mass models on the prediction of synthesis cross sections for superheavy elements. *Phys. Rev. C* **109**, 054611 (2024). <https://doi.org/10.1103/PhysRevC.109.054611>
220. Y. Qiang, X.Q. Deng, Y. Shi et al., Survival probabilities of compound superheavy nuclei towards element 119. (2024). [arXiv:2408.07371](https://arxiv.org/abs/2408.07371)
221. S. Kimura, H. Ishiyama, H. Miyatake et al., Development of the detector system for β -decay spectroscopy at the KEK Isotope Separation System. *Nucl. Instrum. Methods Phys. Res., Sect. B* **376**, 338–340 (2015). <https://doi.org/10.1016/j.nimb.2016.01.041>
222. G.G. Adamian, N.V. Antonenko, A. Diaz-Torres et al., How to extend the chart of nuclides? *Eur. Phys. J. A* **56**, 1–51 (2020). <https://doi.org/10.1140/epja/s10050-020-00046-7>
223. J.M. Gates, G.K. Pang, J.L. Pore et al., First direct measurements of superheavy-element mass numbers. *Phys. Rev. Lett.* **121**, 222501 (2018). <https://doi.org/10.1103/PhysRevLett.121.222501>
224. D. Chandler, D. Hartanto, J.W. Bae et al., *Isotope production and materials irradiation research studies to support HFIR LEU conversion assessment* (Technical report, Oak Ridge National Laboratory (ORNL), Oak Ridge, TN (USA), 2023)
225. J. Werner, W.E. Bickford, D.B. Lord et al., Summary of plutonium-238 production alternatives analysis final report, Technical report, Idaho National Lab. (INL), Idaho Falls, ID (United States) (2013)
226. B. Zhuikov, Production of medical radionuclides in Russia: Status and future—a review. *Appl. Radiat. Isot.* **84**, 48–56 (2014). <https://doi.org/10.1016/j.apradiso.2013.11.025>
227. D. Parrat, G. Bignan, J. Chauvin et al., The future Jules Horowitz material test reactor: a major European research infrastructure for sustaining the international irradiation capacity. in: *9th International Conference on WWER Fuel Performance, Modelling and Experimental Support*, Bulgaria (2011)
228. W. Xu, J. Li, J. Zhao et al., An optimization design study of producing transuranic nuclides in high flux reactor. *Nucl. Eng. Technol.* **55**(8), 2723–2733 (2023). <https://doi.org/10.1016/j.net.2023.04.023>

229. S.G. Nilsson, C.F. Tsang, A. Sobiczewski et al., On the nuclear structure and stability of heavy and superheavy elements. *Nucl. Phys. A* **131**(1), 1–66 (1969). [https://doi.org/10.1016/0375-9474\(69\)90809-4](https://doi.org/10.1016/0375-9474(69)90809-4)
230. R.R. Chasman, I. Ahmad, A.M. Friedman et al., Survey of single-particle states in the mass region $A > 228$. *Rev. Mod. Phys.* **49**(4), 833–891 (1977). <https://doi.org/10.1103/RevModPhys.49.833>
231. J.J. Li, N. Tang, Y.H. Zhang et al., Progress on production cross-sections of unknown nuclei in fusion evaporation reactions and multinucleon transfer reactions. *Int. J. Mod. Phys. E* **32**(01), 2330002 (2023). <https://doi.org/10.1142/S0218301323300023>
232. W.D. Loveland, The synthesis of new neutron-rich heavy nuclei. *Front. Phys.* **7**, 23 (2019). <https://doi.org/10.3389/fphy.2019.00023>
233. B.B. Back, S. Bjørnholm, T. Døssing et al., Relaxation of angular momentum in fission and quasifission reactions. *Phys. Rev. C* **41**, 1495–1511 (1990). <https://doi.org/10.1103/PhysRevC.41.1495>
234. W.Q. Shen, J. Albinski, R. Bock et al., Characteristic time for mass asymmetry relaxation in quasi-fission reactions. *Europhys. Lett.* **1**(3), 113 (1986). <https://doi.org/10.1209/0295-5075/1/3/004>
235. W.Q. Shen, J. Albinski, A. Gobbi et al., Fission and quasifission in U-induced reactions. *Phys. Rev. C* **36**, 115–142 (1987). <https://doi.org/10.1103/PhysRevC.36.115>
236. V.I. Zagrebaev, A.V. Karpov, W. Greiner, Synthesis of superheavy nuclei: obstacles and opportunities. *EPJ Web Conf.* **86**, 00066 (2015). <https://doi.org/10.1051/epjconf/20158600066>
237. E.M. Kozulin, G.N. Knyazheva, A.V. Karpov et al., Detailed study of multinucleon transfer features in the $^{136}\text{Xe} + ^{238}\text{U}$ reaction. *Phys. Rev. C* **109**, 034616 (2024). <https://doi.org/10.1103/PhysRevC.109.034616>
238. T. Mijatović, Multinucleon transfer reactions: a mini-review of recent advances. *Front. Phys.* **10**, 965198 (2022). <https://doi.org/10.3389/fphy.2022.965198>
239. Y. Yano, The RIKEN RI beam factory project: a status report. *Nucl. Instrum. Methods B* **261**(1), 1009–1013 (2007). <https://doi.org/10.1016/j.nimb.2007.04.174>
240. P. Dolegiewicz, R. Ferdinand, X. Ledoux et al., Status of the SPIRAL2 Project, in: *Proceedings, 10th International Particle Accelerator Conference (IPAC'2019)*, 2019, pp. 844–847. <https://doi.org/10.18429/JACoW-IPAC2019-MOPTS005>
241. Y. Chen, Y. Ye, K. Wei, Progress and perspective of the research on exotic structures of unstable nuclei. *Nucl. Tech. (in Chinese)* **46**, 189 (2023). <https://doi.org/10.11889/j.0253-3219.2023.hjs.46.080020>
242. J.J. Li, C. Li, G. Zhang et al., Theoretical study on production of unknown neutron-deficient $^{280-283}\text{Fl}$ and neutron-rich $^{290-292}\text{Fl}$ isotopes by fusion reactions. *Phys. Rev. C* **98**, 014626 (2018). <https://doi.org/10.1103/PhysRevC.98.014626>
243. M.H. Zhang, Y. Zou, M.C. Wang et al., Possibility of reaching the predicted center of the “island of stability” via the radioactive beam-induced fusion reactions. *Nucl. Sci. Tech.* **35**(9), 161 (2024). <https://doi.org/10.1007/s41365-024-01542-x>
244. S. Wuenschel, K. Hagel, M. Barbui et al., Experimental survey of the production of α -decaying heavy elements in $^{238}\text{U} + ^{232}\text{Th}$ reactions at 7.5–6.1 Mev/nucleon. *Phys. Rev. C* **97**, 064602 (2018). <https://doi.org/10.1103/PhysRevC.97.064602>
245. H.M. Devaraja, S. Heinz, O. Beliuskina et al., Observation of new neutron-deficient isotopes with $Z \geq 92$ in multinucleon transfer reactions. *Phys. Lett. B* **748**, 199–203 (2015). <https://doi.org/10.1016/j.physletb.2015.07.006>
246. T. Niwase, Y.X. Watanabe, Y. Hirayama et al., Discovery of new isotope ^{241}U and systematic high-precision atomic mass measurements of neutron-rich Pa–Pu nuclei produced via multinucleon transfer reactions. *Phys. Rev. Lett.* **130**, 132502 (2023). <https://doi.org/10.1103/PhysRevLett.130.132502>
247. Z.H. Liao, L. Zhu, Z.P. Gao et al., Optimal detection angles for producing $N = 126$ neutron-rich isotones in multinucleon transfer reactions. *Phys. Rev. Res.* **5**, L022021 (2023). <https://doi.org/10.1103/PhysRevResearch.5.L022021>
248. X. Jiang, N. Wang, Probing the production mechanism of neutron-rich nuclei in multinucleon transfer reactions. *Phys. Rev. C* **101**, 014604 (2020). <https://doi.org/10.1103/PhysRevC.101.014604>
249. X.J. Bao, S.Q. Guo, J.Q. Li et al., Influence of neutron excess of projectile on multinucleon transfer reactions. *Phys. Lett. B* **785**, 221–225 (2018). <https://doi.org/10.1016/j.physletb.2018.08.049>
250. Z.Q. Feng, Effect of cluster transfer on the production of neutron-rich nuclides near $N = 126$ in multinucleon-transfer reactions. *Phys. Rev. C* **108**, L051601 (2023). <https://doi.org/10.1103/PhysRevC.108.L051601>
251. G. Zhang, J.J. Li, X.R. Zhang et al., Role of the Guasifission yields in the multinucleon transfer reactions of $^{136}\text{Xe} + ^{208}\text{Pb}$. *Phys. Rev. C* **102**, 024617 (2020). <https://doi.org/10.1103/PhysRevC.102.024617>
252. C. Li, F.S. Zhang, J.J. Li et al., Multinucleon transfer in the $^{136}\text{Xe} + ^{208}\text{Pb}$ reaction. *Phys. Rev. C* **93**, 014618 (2016). <https://doi.org/10.1103/PhysRevC.93.014618>
253. R. Yanez, W. Loveland, Predicting the production of neutron-rich heavy nuclei in multinucleon transfer reactions using a semi-classical model including evaporation and fission competition. GRAZING-F. *Phys. Rev. C* **91**, 044608 (2015). <https://doi.org/10.1103/PhysRevC.91.044608>
254. J.S. Barrett, W. Loveland, R. Yanez et al., $^{136}\text{Xe} + ^{208}\text{Pb}$ reaction: a test of models of multinucleon transfer reactions. *Phys. Rev. C* **91**, 064615 (2015). <https://doi.org/10.1103/PhysRevC.91.064615>
255. Y.H. Zhang, J.J. Li, C. Li et al., Microscopic study of the production of neutron-rich isotopes near $N = 126$ in the multinucleon transfer reactions $^{78,82,86}\text{Kr} + ^{208}\text{Pb}$. *Phys. Rev. C* **109**, 044617 (2024). <https://doi.org/10.1103/PhysRevC.109.044617>
256. N. Wang, L. Guo, New neutron-rich isotope production in $^{154}\text{Sm} + ^{160}\text{Gd}$. *Phys. Lett. B* **760**, 236–241 (2016). <https://doi.org/10.1016/j.physletb.2016.06.073>
257. V. Saiko, A. Karpov, Multinucleon transfer as a method for production of new heavy neutron-enriched isotopes of transuranium elements. *Eur. Phys. J. A* **58**(3), 41 (2022). <https://doi.org/10.1140/epja/s10050-022-00688-9>
258. A. Karpov, V. Saiko, Synthesis of transuranium nuclei in multinucleon transfer reactions at near-barrier energies. *Phys. Part. Nucl. Lett.* **16**(6), 667–670 (2019). <https://doi.org/10.1134/S154747119060475>
259. D.D. Zhang, D. Vretenar, T. Nikšić et al., Multinucleon transfer with time-dependent covariant density functional theory. *Phys. Rev. C* **109**, 024614 (2024). <https://doi.org/10.1103/PhysRevC.109.024614>
260. Z.J. Wu, L. Guo, Production of proton-rich actinide nuclei in the multinucleon transfer reaction $^{58}\text{Ni} + ^{232}\text{Th}$. *Sci. Chin. Phys. Mech.* **63**(4), 242021 (2020). <https://doi.org/10.1007/s11433-019-1484-0>
261. K. Sekizawa, S. Ayik, Quantal diffusion approach for multinucleon transfer processes in the $^{58,64}\text{Ni} + ^{208}\text{Pb}$ reactions: Toward the production of unknown neutron-rich nuclei. *Phys. Rev. C* **102**, 014620 (2020). <https://doi.org/10.1103/PhysRevC.102.014620>
262. K. Sekizawa, Enhanced nucleon transfer in tip collisions of $^{238}\text{U} + ^{124}\text{Sn}$. *Phys. Rev. C* **96**, 041601 (2017). <https://doi.org/10.1103/PhysRevC.96.041601>

263. A. Kayaalp, M. Arik, S. Ocal et al., A quantal diffusion approach for multinucleon transfer in heavy-ion collisions. *Nucl. Phys. A* **1050**, 122916 (2024). <https://doi.org/10.1016/j.nuclphysa.2024.122916>
264. B.J. Roy, S. Santra, A. Pal et al., Reaction mechanism study for multinucleon transfer processes in collisions of spherical and deformed nuclei at energies near and above the Coulomb barrier: The $^{16}\text{O} + ^{154}\text{Sm}$ reaction. *Phys. Rev. C* **105**, 044611 (2022). <https://doi.org/10.1103/PhysRevC.105.044611>
265. G. Zhang, C.A.T. Sokhna, Z. Liu et al., Production of neutron-rich isotopes $^{264,266,268,269}\text{Rf}$ by multinucleon transfer reactions based on ^{238}U beam. *Phys. Rev. C* **100**, 024613 (2019). <https://doi.org/10.1103/PhysRevC.100.024613>
266. P.W. Wen, C. Li, L. Zhu et al., Mechanism of multinucleon transfer reaction based on the GRAZING model and DNS model. *J. Phys. G Nucl. Part. Phys.* **44**(11), 115101 (2017). <https://doi.org/10.1088/1361-6471/aa8b07>
267. L. Zhu, J. Su, C. Li et al., How to approach the island of stability: reactions using multinucleon transfer or radioactive neutron-rich beams? *Phys. Lett. B* **829**, 137113 (2022). <https://doi.org/10.1016/j.physletb.2022.137113>
268. K. Zhao, Z.X. Li, N. Wang et al., Production mechanism of neutron-rich transuranium nuclei in $^{238}\text{U} + ^{238}\text{U}$ collisions at near-barrier energies. *Phys. Rev. C* **92**, 024613 (2015). <https://doi.org/10.1103/PhysRevC.92.024613>
269. V.V. Saiko, A.V. Karpov, Analysis of multinucleon transfer reactions with spherical and statically deformed nuclei using a Langevin-type approach. *Phys. Rev. C* **99**, 014613 (2019). <https://doi.org/10.1103/PhysRevC.99.014613>
270. L. Zhu, New model based on coupling the Master and Langevin equations in the study of multinucleon transfer reactions. *Phys. Lett. B* **849**, 138423 (2024). <https://doi.org/10.1016/j.physletb.2023.138423>
271. F.C. Dai, P.W. Wen, C.J. Lin et al., Theoretical study of multinucleon transfer reactions by coupling the Langevin dynamics iteratively with the master equation. *Phys. Rev. C* **109**, 024617 (2024). <https://doi.org/10.1103/PhysRevC.109.024617>
272. V.V. Saiko, A.V. Karpov, Production of neutron-enriched isotopes along magic number $N = 126$ by multinucleon transfer reactions with radioactive-ion beams. *Phys. Rev. C* **109**, 064607 (2024). <https://doi.org/10.1103/PhysRevC.109.064607>
273. P.H. Chen, F. Niu, W. Zuo et al., Approaching the neutron-rich heavy and superheavy nuclei by multinucleon transfer reactions with radioactive isotopes. *Phys. Rev. C* **101**, 024610 (2020). <https://doi.org/10.1103/PhysRevC.101.024610>
274. C. Li, P.W. Wen, J.J. Li et al., Production of heavy neutron-rich nuclei with radioactive beams in multinucleon transfer reactions. *Nucl. Sci. Tech.* **28**(8), 110 (2017). <https://doi.org/10.1007/s41365-017-0266-z>
275. M.H. Mun, G.G. Adamian, N.V. Antonenko et al., Toward neutron-rich nuclei via transfer reactions with stable and radioactive beams. *Phys. Rev. C* **91**, 054610 (2015). <https://doi.org/10.1103/PhysRevC.91.054610>

Springer Nature or its licensor (e.g. a society or other partner) holds exclusive rights to this article under a publishing agreement with the author(s) or other rightsholder(s); author self-archiving of the accepted manuscript version of this article is solely governed by the terms of such publishing agreement and applicable law.